CRC Report No. A-111

IMPROVING WEST COAST OZONE BOUNDARY CONDITIONS FOR REGIONAL AIR QUALITY MODELS

APRIL 2019

COORDINATING RESEARCH COUNCIL, INC.

5755 NORTH POINT PARKWAY • SUITE 265 • ALPHARETTA, GA 30022

The Coordinating Research Council, Inc. (CRC) is a non-profit corporation supported by the petroleum and automotive equipment industries. CRC operates through the committees made up of technical experts from industry and government who voluntarily participate. The four main areas of research within CRC are: air pollution (atmospheric and engineering studies); aviation fuels, lubricants, and equipment performance; heavy-duty vehicle fuels, lubricants, and equipment performance (e.g., diesel trucks); and light-duty vehicle fuels, lubricants, and equipment performance (e.g., passenger cars). CRC's function is to provide the mechanism for joint research conducted by the two industries that will help in determining the optimum combination of petroleum products and automotive equipment. CRC's work is limited to research that is mutually beneficial to the two industries involved. The final results of the research conducted by, or under the auspices of, CRC are available to the public.

CRC makes no warranty expressed or implied on the application of information contained in this report. In formulating and approving reports, the appropriate committee of the Coordinating Research Council, Inc. has not investigated or considered patents which may apply to the subject matter. Prospective users of the report are responsible for protecting themselves against liability for infringement of patents.

Improving West Coast Ozone Boundary Conditions for Regional Air Quality Models

Final Report

Prepared for:
Bay Area Air Quality Management District
375 Beale Street, Suite 600
San Francisco, CA 94105

California Air Resources Board
2828, 1001 I Street
Sacramento, CA 95814

Coordinating Research Council
5755 North Point Parkway, Suite 265
Alpharetta, GA 30022

Prepared by:
Chris Emery, Marco Rodriguez, Chao-Jung Chien
Ramboll Environment and Health
7250 Redwood Boulevard, Suite 105
Novato, CA 94945

With contributions from:
David Fairley, Su-Tzai Soong, Bonyoung Koo,
Steve Reid, Jeff Matsuoka, Saffet Tanrikulu
Bay Area Air Quality Management District

www.ramboll.com
415-899-0700

April 2019
1690005972

CONTENTS

TABLES

FIGURES

EXECUTIVE SUMMARY

The lateral boundaries of regional air quality models applied over the western US often extend over the Pacific Ocean. Historically, boundary conditions have been developed in several ways, each with its own degree of uncertainty. The use of global models to derive regional boundary conditions is much more effective and promising than previous approaches based entirely on simplistic assumptions or limited observational data. Nevertheless, recent modeling conducted by the Bay Area Air Quality Management District (BAAQMD) shows that uncertainty in western boundary conditions impacts both the model's ability to replicate measured air quality patterns and the model's response to emission reductions. As US emissions have decreased while contributions from international transport have increased over the past 20 years, it has become increasingly important to properly characterize boundary conditions entering the domain from the northeastern Pacific Ocean.

In this project, Ramboll and the BAAQMD developed a method to reduce regional biases in global model-derived ozone fields over the northeastern Pacific Ocean using routine ozonesonde measurements. The method was codified into a distributable software tool that can be used to adjust regional ozone boundary conditions derived from the Model of Ozone and Related Tracers (MOZART) global model over the period 2012-2016 for modeling domains extending beyond the US west coast. This effort will benefit western US regional air quality model applications that support both regulatory and research-oriented projects.

MOZART has been run operationally by the National Center of Atmospheric Research (NCAR). Ramboll retrieved 6-hourly gridded output over 2012-2016; weekly ozonesonde data from Trinidad Head, California was also retrieved for the same period. The BAAQMD conducted a statistical classification analysis from which to derive a regression-based parameterized model that reduces MOZART-measurement biases on a daily basis. Ramboll then developed a file of adjusted ozone concentration profiles for each day of the 5-year period for use in a Python-based tool that replaces ozone values in regional model boundary condition files within user-defined portions of the model domain. Ramboll developed the adjustment program to be flexible so that adjustments from regression models developed for other years can be readily incorporated in the future.

The BAAQMD applied the adjustment tool to their 2016 daily ozone boundary condition (BC) input files and ran their Community Multi-scale Air Quality (CMAQ) modeling system for an initial test in which the northern half of the western boundary was modified between the surface and ~5000 m. In an alternative test, the BC adjustment was applied to the northern two-thirds of the western boundary and to the western one-third of the northern boundary (same vertical adjustment). Results were analyzed graphically and statistically over the ozone season (May-October). Two basic paradigms were identified: (1) Increased BCs aloft mix down during the day over high-elevation topography, then disperse at the surface to other area of the domain; (2) reduced BCs in the marine boundary layer are transported along the coastline in the consistent northwesterly flow and occasionally drawn through coastal topographic gaps such as the Bay Area.

Comparisons against ozonesonde data showed little impact on CMAQ overpredictions of ozone in the marine boundary layer but large reductions in median ozone underpredictions aloft, as would be expected with the regression model's attempt to adjust BC ozone toward seasonal means. Overall, impacts to statistical performance throughout the ozonesonde column were minor. The Half Moon Bay ozonesonde tended to be less influenced by the choice of ozone BCs than the more northern Bodega Bay site, which may be caused by a somewhat stronger local influence from the Bay Area and/or more influence from unadjusted portions of the western boundary.

At surface monitors in the Bay Area and Central Valley, the effects of the ozone BC adjustment were rather small and difficult to differentiate except for a few scattered days, with a tendency for more evident impacts at the inland and southern Bay Area sites. In the Bay Area, the adjusted ozone BC simulation slightly raised ozone, thereby raising the overprediction bias and gross error by a few percentage points. In the Central Valley, the adjusted ozone BC simulation slightly raised ozone, thereby improving the underprediction bias by a few percentage points. Overall, however, we found no significant change in model performance statistics or CMAQ's characterization of hourly ozone with the ozone BC adjustment. Results suggest that areas in elevated terrain along the western US coast may be more affected by boundary condition adjustments than low-level sites. Ozone levels in 2016 were relatively low compared to other years, and BC adjustments may have larger or smaller impacts in other years.

The tool developed in this project is now available to further investigate and test additional boundary condition modifications and adjustments. While the use of global models is more effective and promising than previous approaches, they introduce their own biases and errors when their results are down-scaled for regional modeling applications. Our approach to remove these biases using a mix of model and observational data, while effective to first order, also reduces concentration variability at all altitudes (i.e., higher-order structures). Furthermore, regional model performance may be more affected by the proximity of boundary conditions to the western shoreline. We recommend future work that locates grid boundaries farther away from the coastline to minimize BC impacts. The tool developed in this project can help determine regional model sensitivity to boundary placement.

1.0 INTRODUCTION

The lateral boundaries of regional air quality models applied over the western US often extend over the Pacific Ocean. Historically, boundary conditions have been developed from one of four data sources: (1) a set of “default” or “typical” background vertical concentration profiles; (2) aircraft measurements from special field study missions; (3) routine surface and sounding measurements; and now most commonly, (4) global model output. While satellite-derived profiles are a potentially valuable resource in the future, current data products possess much uncertainty and provide insufficient vertical resolution in the troposphere.

Each of the four methods above introduces a large degree of uncertainty. For example, EPA’s default vertical profiles are now considered obsolete, provide no horizontal variation, and represent decades-old historical conditions more typical of the continental eastern US. Data obtained from aircraft missions are sparse in time and space, and typically noisy. Routine surface and sounding measurements are spatially sparse, mostly located well inland, and thus not necessarily representative of concentrations over the Pacific Ocean. Global models, which address intercontinental chemistry and transport, possess rather coarse temporal and spatial resolution (e.g., 3- or 6-hourly, ~300 km grid spacing) and exhibit their own biases that typically include ozone overestimates in the marine boundary layer.

Recent modeling conducted by the Bay Area Air Quality Management District (BAAQMD) shows that uncertainty in western boundary conditions impacts both the model’s ability to replicate measured air quality patterns and the model’s response to emission reductions. On a climatological basis, during much of the year lower tropospheric air entering northern and southern California originates over the northeastern Pacific as it circulates anticyclonically around the semi-permanent eastern Pacific subtropical high pressure system. As US emissions have decreased while contributions from international transport have increased over the past 20 years, it has become increasingly important to properly characterize boundary conditions entering the western US at all altitudes.

This report describes a project jointly conducted by Ramboll and the BAAQMD to develop and demonstrate a method to improve the characterization of global model-derived ozone fields over the northeastern Pacific Ocean using routine ozone measurements. The method has been codified into a distributable software tool that can be used to adjust regional ozone boundary conditions for any modeling domain extending beyond the US west coast. This effort will benefit western US regional air quality model applications that support both regulatory and research-oriented projects. This project was jointly funded by the BAAQMD, the California Air Resources Board, and the Coordinating Research Council.

2.0 DATA AND METHODOLOGY

The National Center for Atmospheric Research (NCAR) has routinely run the global Model for Ozone and Related Tracers (MOZART; Emmons et al., 2010) on a daily operational basis and provides 6-hourly model output between 2006 and 2017. These MOZART datasets have been commonly used to develop boundary conditions for regional photochemical modeling in the US. Beginning in winter 2017/18, NCAR has been running a replacement global model called the Whole Atmosphere Community Climate Model (WACCM; Marsh et al., 2013) and posting output from daily 72-hour forecast cycles, which is similar in format and content to MOZART.

For this study, Ramboll retrieved MOZART data for an entire 5-year period (January 2012 through December 2016). This period includes the BAAQMD's modeling years of 2012 and 2016 and the summer 2016 California Baseline Ozone Transport Study (CABOTS). Ramboll also obtained routine ozone profile data from the Trinidad Head monitoring site on the northern California coast (NOAA, 2019) for the same period. Ramboll statistically compared MOZART ozone fields against those observations to characterize seasonal biases and variability. Using the full 5-year datasets, the BAAQMD conducted a statistical classification analysis involving MOZART and measured ozone profiles and routine upper-air meteorological data, from which to derive a regression-based parameterized model that reduces overall MOZART-measurement biases on a daily basis.

Ramboll then developed a file of regression model-based adjusted ozone concentration profiles for each day of the 2012-2016 period. This file provides ozone values for each MOZART vertical layer from the surface to ~5000 m altitude; values are taken from the regression model on days that Trinidad Head ozonesonde data are not available, and from direct substitution of Trinidad Head ozonesonde data on days those profiles are available. Ramboll developed a Python-based tool that replaces ozone values in CMAQ boundary condition files within user-defined portions of the model domain. Note that this program should only be applied to regional boundary conditions extending over the Pacific Ocean and that have been developed from MOZART data within the 2012-2016 analysis period. Ramboll has developed the adjustment program to be flexible so that adjustments from regression models developed for other years can be readily incorporated in the future.

Details of the approach and results are described in the following subsections.

2.1 Data Sources

Ramboll considered the use of multiple sources of measurement data to support the project. Selection criteria were necessarily strict, including the need for routine ozone monitoring at fixed locations, a high level of data completeness over the period of interest, and a focus on rural locations along the western US coast that in particular would adequately represent ozone concentrations in lower tropospheric air with origins over the northeastern Pacific Ocean. This ruled out urban-oriented sites associated with the EPA's Air Quality System (AQS) network.

Figure 1 shows a map of the few measurement sites that met at least a few of our criteria. Routine rural surface monitoring sites include those reporting to the Clean Air Status and Trends Network (CASTNET): Mount Rainier (MOR); Lassen (LAV); Pinnacles (PIN); Yosemite (YOS) and Joshua Tree (JOT). Sites at higher elevations and/or including vertical soundings include the Mt. Bachelor Observatory (MBO) in Oregon, the tropospheric lidar ozone profiler at the Table Mountain Facility (TMF) in Southern California, and the ozonesonde site at Trinidad Head (THD) on the northwestern California coastline.

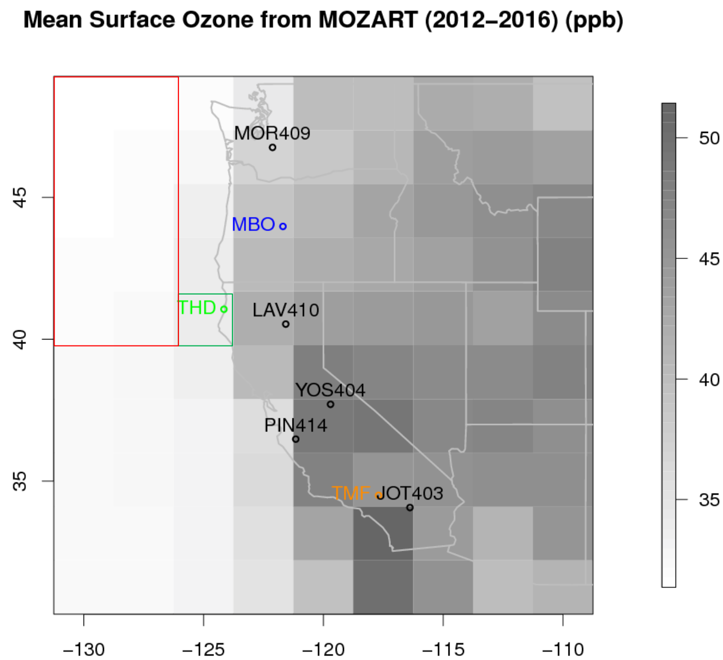

Figure 1. Mean surface gridded ozone (ppb) predicted by MOZART over 2012-2016, including candidate ozone monitoring sites (surface sites in black, elevated/profiler sites colored) and the 10-cell MOZART grid area (red outline) used to compare predicted ozone profiles against observed profiles at THD.

To illustrate the influence of continental emissions on ozone patterns over the western US, Figure 1 overlays a “tile plot” of gridded MOZART-generated mean surface ozone concentrations during the 2012-2016 period; the coarse resolution of the MOZART grid is evident in the Figure. Ozone at all surface CASTNET sites in Figure 1 are clearly influenced to varying degrees by local emissions and are thus not appropriate for assessing MOZART-derived ozone concentrations entering the US from the eastern Pacific. Although the TMF site is located at an altitude of just over 2 km in the mountains northeast of Los Angeles and it reports deep tropospheric ozone profiles, lower tropospheric air at TMF is influenced by urban emissions from Southern California and by longer-range transport of air traversing northern California and inland deserts.

On the other hand, we would expect the THD ozonesonde site would be least influenced by continental sources in the marine boundary layer, both in terms of frequency and magnitude. Additionally, any continental influence should rapidly decrease with altitude as winds in the mid and upper troposphere are increasingly westerly and thus bring a more substantial contribution from global background and international transport. A similar argument could be made for MBO, given its proximity to THD and its siting on a Cascade Mountain summit (~3 km), which conceivably measures mid-tropospheric air with similar origins as sensed by the THD ozonesonde profiles. The fact that THD ozonesondes are launched roughly once per week presents the single disadvantage with these data. While MBO reports hourly data, it monitors at a single fixed altitude, limiting its usefulness for this project. We elected to use MBO data in this project to gauge consistency with THD-MOZART comparisons at similar altitudes.

2.2 MOZART-Observation Comparisons

Figure 2 presents a graphical comparison of seasonally-averaged ozone profiles and their variability as predicted by MOZART and observed at THD over the entire 2012-2016 period. MOZART profiles were generated from a 10-cell average over the eastern Pacific (Figure 1), which represents a general source area from which lower tropospheric air conceivably flows into the US west coast as it circulates around the eastern Pacific subtropical high pressure system. Therefore, this same area represents the source of low- and mid-tropospheric boundary condition ozone in western US modeling exercises. MOZART profiles were extracted on the days and nearest time (18 UTC) when THD profiles were available. THD data were averaged to the MOZART vertical grid for visual consistency.

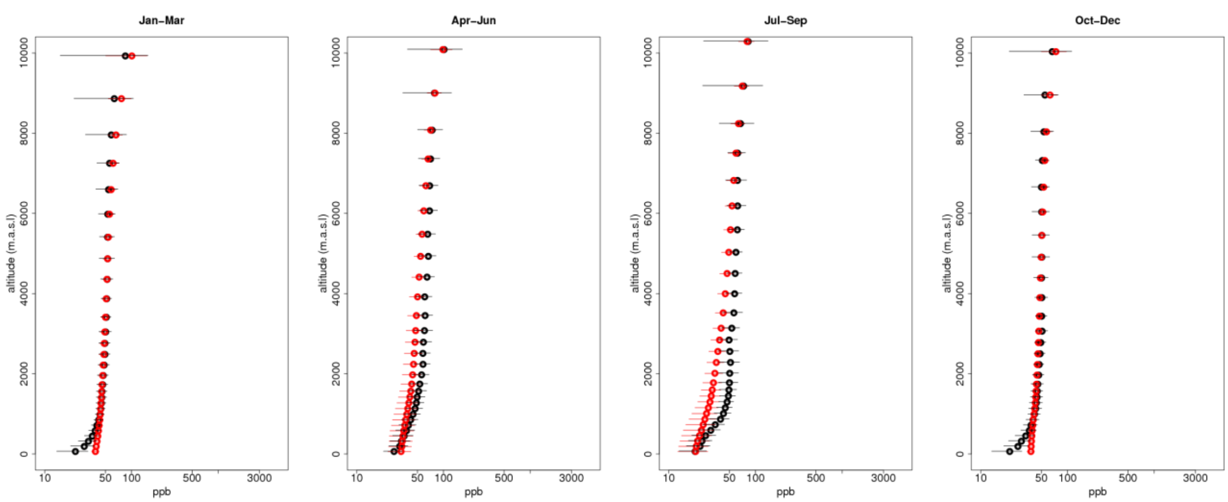

Figure 2. 2012-2016 seasonal THD observed (black) and MOZART predicted (red) ozone profiles over the 10-cell area shown in Figure 1. Dots represent seasonally-averaged values on days when THD profiles were available, whiskers represent standard deviations.

Initial inspection of Figure 2 indicates generally good agreement between model and measurements each season over the 5-year period. But certain consistent differences are exposed: (1) MOZART exhibits much less variability than observed over all altitudes and seasons, but especially above 6 km where seasonal tropospheric-stratospheric exchange processes are evident; (2) MOZART tends to overpredict ozone in the marine boundary layer (<500 m), especially in winter and autumn; and (3) MOZART tends to underpredict ozone between 500 m and 6 km, especially in spring and summer. The boundary layer overprediction is likely related to several factors: (1) the MOZART grid cannot adequately resolve the large coastal gradient of continental emissions, which may raise ozone in near-shore grid cells; (2) predictions are likely subject to large numerical diffusion of continental ozone directed offshore; and (3) MOZART chemistry lacks a complete destruction mechanism (e.g., via oceanic halogens) and may overestimate production efficiency from sources such as shipping NOx.

Figure 3 presents seasonal scatter plots comparing MOZART and THD ozone based on the same data used for Figure 2. Plots are separated by season and three altitude ranges: 0-1000 m, 1000-5000 m, and 5000-10000 m. These comparisons reveal a large degree of scatter with roughly equivalent variability among both MOZART and THD in the lower troposphere during most seasons. Winter/fall boundary layer overpredictions, and spring/summer mid-troposphere underpredictions are evident. While model-observation agreement is much more correlated in the upper troposphere, the model lacks observed variability. Figure 4 presents the same data as probability density functions of model-observation differences (or model error), and many of the same features described above are evident.

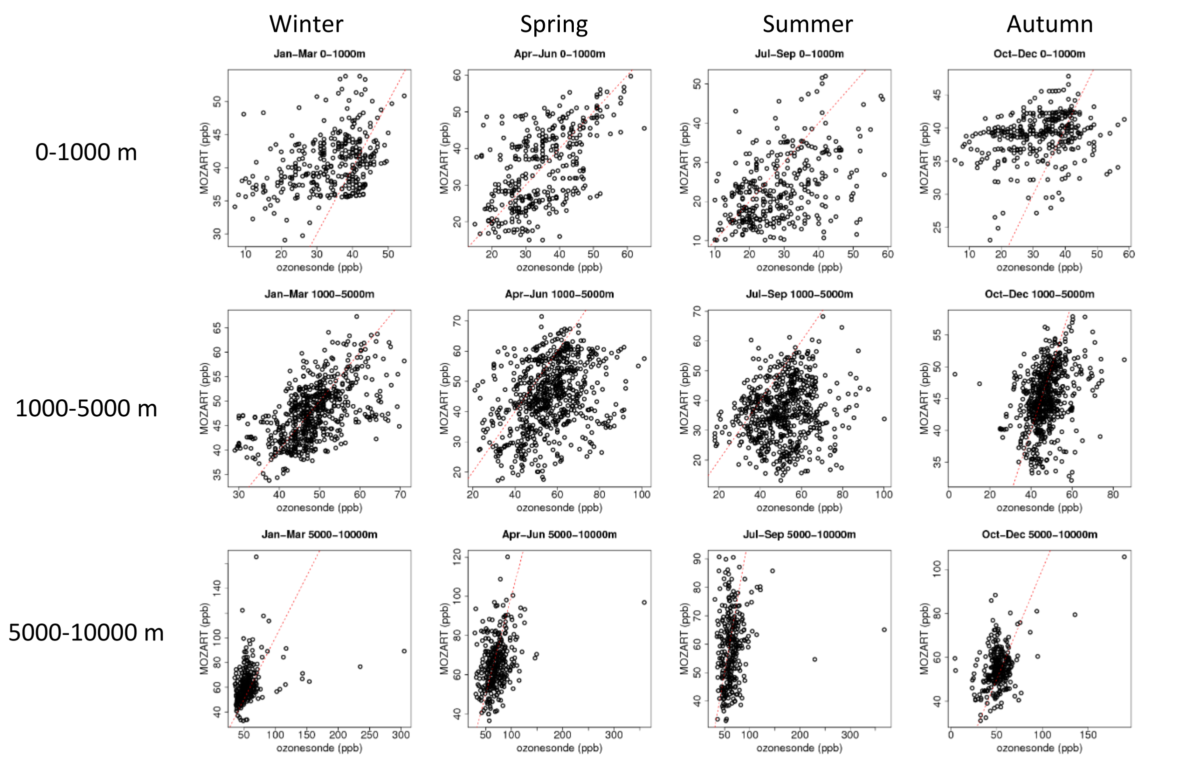

Figure 3. Scatter plots of MOZART-predicted vs. THD observed ozone by season and altitude over the 2012-2016 analysis period. The 1:1 correspondence is shown as a red-dash line.

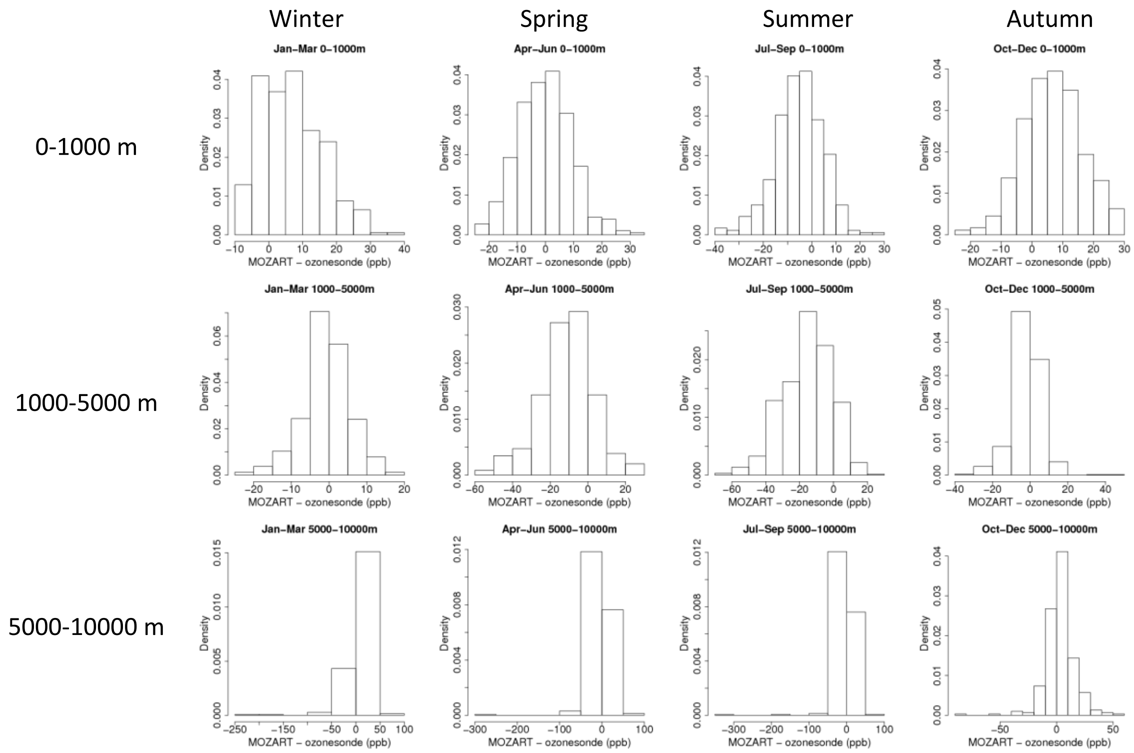

Figure 4. Probability density functions of MOZART ozone prediction errors relative to THD observations by season and altitude over the 2012-2016 analysis period.

Figure 5 shows similar plots as Figures 3 and 4, but for MOZART-MBO ozone comparisons. These results confirm consistent agreement with THD plots for 1000-5000 m altitude range, but with perhaps a wider range of scatter and model error because of the much larger number of data pairs available with MBO. Statistics noted on the scatter plots indicate that MOZART and MBO means and standard deviations are very similar, with standard deviations ranging 10-20% of the mean values.

In conclusion, all of these comparisons show that MOZART is able to replicate seasonal mean concentrations at most altitudes rather well, but the model does exhibit certain consistent biases in the lower troposphere that can reach 20-30 ppb seasonally, and exhibits much less variability in the upper troposphere.

2.3 Regression Model Development

The BAAQMD identified vertical ranges in the MOZART 10-cell average ozone column profiles where predictions consistently and substantially differ from THD profiles. For each of those ranges, BAAQMD developed regression-based adjustment formulas using combinations of MOZART predictions, meteorological sounding data, and temporal parameters as covariates that minimize the systematic biases. The approach employed a statistical multi-variate cluster analysis that finds an optimal combination of variables and coefficients to form a linear function

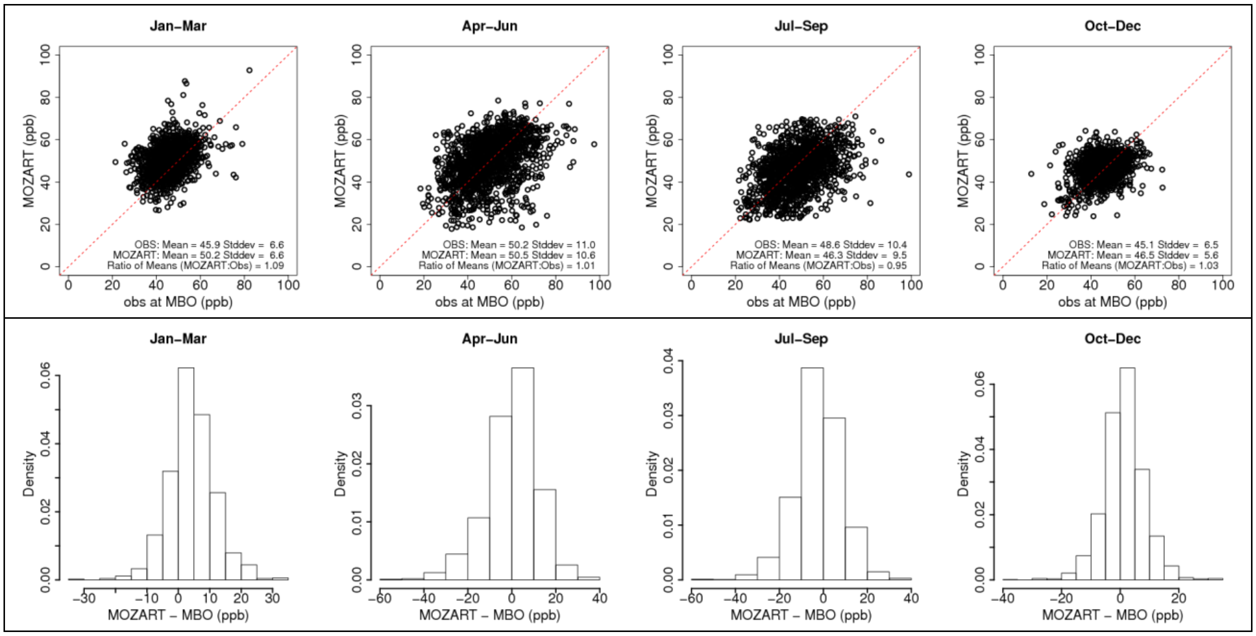

Figure 5. Scatter plots (top) and probability density functions (bottom) of MOZART-predicted vs. MBO observed ozone by season over the 2012-2016 analysis period. The 1:1 correspondence is shown as a red-dash line in the top plots.

of factors that minimizes MOZART-THD deviations in each layer and for each day during 2012-2016.

We want an ozone estimate to both be unbiased and not deviate greatly around what it seeks to estimate or, using other terminology, we want an estimate to be both precise and accurate. Mean squared error (MSE) is a metric that measures both precision and accuracy by incorporating systematic bias (or mean difference) and unsystematic variance (or variability from the mean). If *Xo* is the ozonesonde value and *Xm* is the corresponding MOZART estimate, then:

$$MSE = E(Xm - Xo)^2 = [E(Xm - Xo)]^2 + E(Xm - \overline{Xm})^2 = Bias^2 + Variance$$

Relative MSE is normalized by the mean THD observation over the entire dataset. We assume that the ozonesonde measurements have little or no bias and that ozonesonde measurement error is of much smaller magnitude than the MOZART prediction variance.

Figure 6 shows profiles of absolute (unsigned) relative bias and the square root of relative MSE (RMSE) over the entire data period. MOZART consistently overestimates THD in the lowest 5 layers (~500 m), with moderate to high bias and MSE. MOZART consistently underestimates THD in layers 6-22 (~500-5000 m), with moderate bias and MSE. Near layer 30 (~10,000 m) MOZART has low bias but high MSE (i.e., high variance), which we attribute to modeling uncertainties related to resolving the tropopause location. In other words, MOZART can replicate the mean THD observation at that altitude over the data period, but cannot replicate

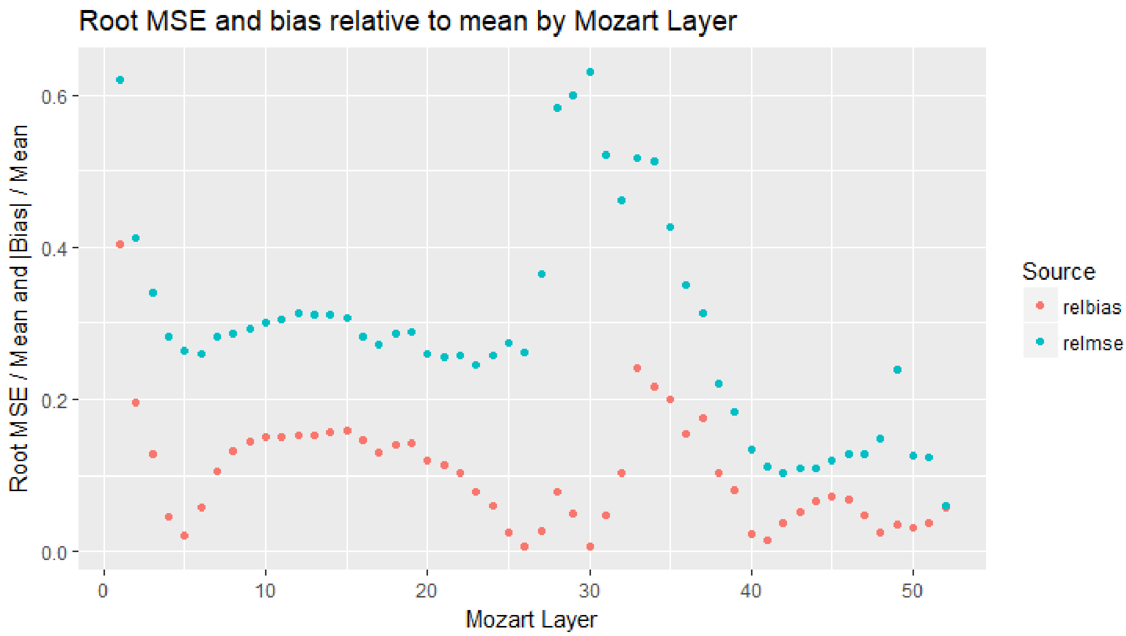

Figure 6. Profiles of absolute (unsigned) relative bias (red) and the square root of relative MSE (RMSE, blue) between MOZART predicted ozone and THD observed ozone on days THD data were available over the entire data period of 2012-2016.

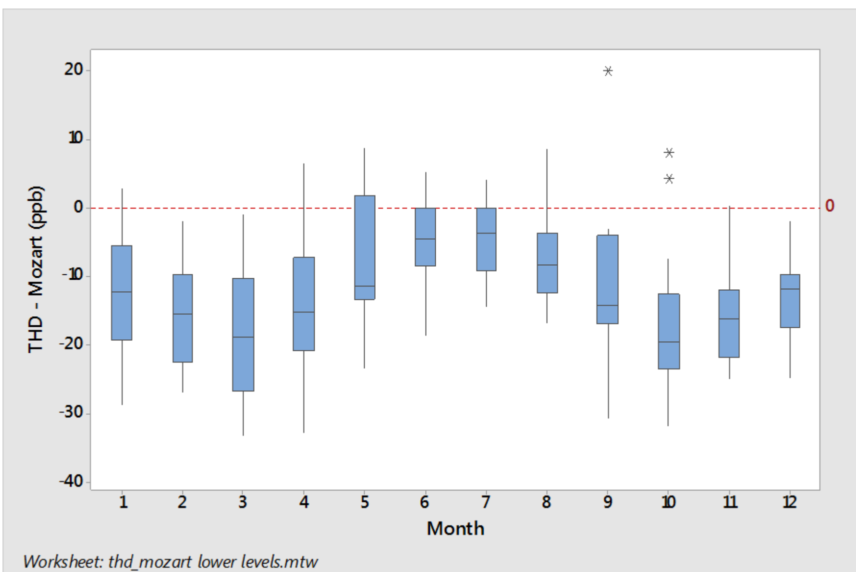

Figure 7. Monthly distributions of MOZART-THD ozone differences in MOZART layers 1-5: boxes represent the interquartile range; lines within the boxes represent means, whiskers represent the 90th percentile range; asterisks represent maxima.

its variability. This unsystematic variance around the tropopause was considered less important and not addressed in this study. Figure 7 shows the monthly distributions of MOZART-THD ozone differences in layers 1-5 as box and whisker plots. The late winter and autumn overpredictions are evident, with much smaller differences in summer months. The difference pattern over the year exhibits a definite wave pattern, which is considered in the regression model described below.

In developing separate regression models for the two regions spanning layers 1-5 and 6-22, we tried various combinations of meteorological predictors from local off-shore buoys, local routine airport observations, and twice-daily regional radiosonde (RAOB) sites. From this process we found that local surface-based meteorological data were of only marginal utility. However, certain Medford RAOB parameters reported at 925 and 850 mb pressure levels provided a useful dataset for regression, which was aided by the fact that there were very few missing data. Medford is located 180 km northeast of Trinidad Head in southwestern Oregon. Therefore, the regression model centered on MOZART predictions, Medford RAOB parameters, and a set of wave functions to capture four modes of intra-annual variability each year. Since THD profiles are measured roughly once/week around midday local time, the regression model was provided 10-cell average MOZART ozone profiles (Figure 1) from the 18:00 UTC output fields.

We found little ozone trend in the THD data beyond a single year, so the regression models account only for intra-year variations (according to annual wave numbers 1 through 4). Although THD data provide no information on diurnal patterns, we analyzed temporal patterns in MOZART 6-hourly ozone concentrations and found no practical significance for the over-ocean grid cells. Thus, to first approximation, these regression equations apply for all periods during the day.

Table 1 shows the best-fit regression model for MOZART layers 1-5. This model includes 11 variables per layer, including MOZART mean ozone, 6 Medford RAOB variables (925 and 850 mb heights, temperature, dewpoint, and wind speed), and 4 sine/cosine terms of modes 1, 2 and 3. The generalized regression model for predicted ozone in layer *l*, on a given Julian date *d* is:

$$p(l,d) = m(l) + b_1[x_1(l,d) - c_1(l)] + b_2[x_2(d) - c_2] + \cdots + b_{11}[x_{11}(d) - c_{11}]$$

The coefficient of determination (denoted by R^2), a key metric in regression analysis, is the fraction of variance in the dependent variable that is predictable from the independent variable. In this case, the R^2 shows the improvement in fit compared with predicting THD ozone from its mean value. For these lowest levels, the reduction in MSE was found to be considerably larger than the model-adjusted R^2 because just adjusting for bias reduced the MSE considerably. The regression RMSE was 6.2 ppb, a reduction of nearly half from the unadjusted RMSE of 11 ppb. The regression R^2 was 57% from an unadjusted R^2 of ~30%. Figure 8 shows an example of MOZART-THD comparisons with and without the regression model adjustment.

Table 2 shows the best-fit regression model for MOZART layers 6-22. This simpler model includes 9 variables per layer, including MOZART mean ozone and all 8 sine/cosine terms of modes 1 through 4. The generalized regression model for predicted ozone in layer *l*, on a given Julian date *d* is:

Table 1. Best-fit regression model of 11 parameters and coefficients for MOZART layers 1-5 over 2012-2016.

Variable Name	Variable	Center (c_i)	Coefficient (b_i)
MOZART ozone (ppb)	x_1	See below	0.303
Medford 850 mb height (meters)	x_2	1500	-0.038
Medford 850 mb temperature (10xC)	x_3	77	-0.0363
Medford 850 mb windspeed (m/s)	x_4	47	0.0467
Medford 925 mb temperature (10xC)	x_5	100	0.0552
Medford 925 mb dewpoint (10xC)	x_6	40	-0.0481
Medford 925 mb windspeed (m/s)	x_7	24	0.0347
sin(1x2πd/365)	x_8	0	1.17
cos(1x2πd/365)	x_9	0	-1.87
sin(2x2πd/365)	x_{10}	0	-1.48
cos(3x2πd/365)	x_{11}	0	1.58

Layer-Specific Ozone	$c_1(l)$	$m(l)$
Layer 1	32.25	22.33
Layer 2	32.75	26.66
Layer 3	33.36	28.88
Layer 4	34.05	31.91
Layer 5	34.84	34.94

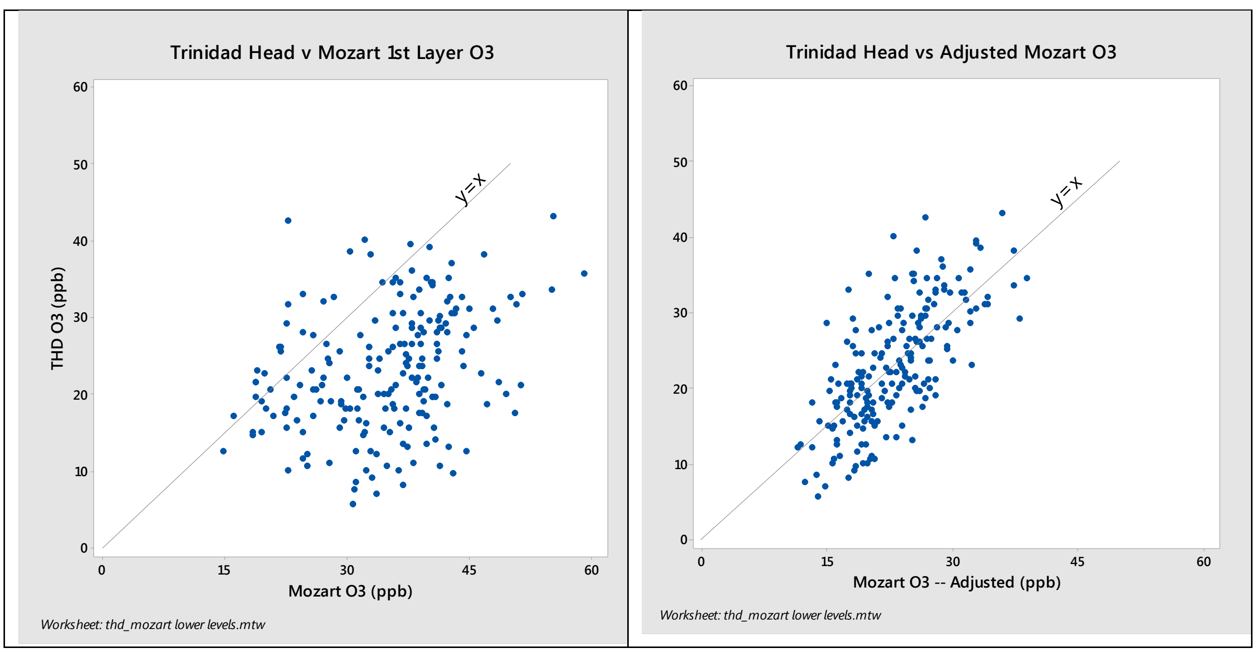

Figure 8. Comparison of MOZART-THD comparison (model layer 1) for all days when THD ozonesonde data are available over 2012-2016: (Left) unadjusted MOZART values; (Right) regression adjusted MOZART values. Note that THD data are referenced to the y-axis, while MOZART data are referenced to the x-axis.

Table 2. Best-fit regression model of 9 parameters and coefficients for MOZART layers 6-22 over 2012-2016.

Variable Name	Variable	Center (c_i)	Coefficient (b_i)
MOZART ozone (ppb)	x_1	See below	0.361
sin(1x2πd/365)	x_2	0	0.794
cos(1x2πd/365)	x_3	0	-5.589
sin(2x2πd/365)	x_4	0	-0.413
cos(2x2πd/365)	x_5	0	0.609
sin(3x2πd/365)	x_6	0	-0.667
cos(3x2πd/365)	x_7	0	0.875
sin(4x2πd/365)	x_8	0	0.461
cos(4x2πd/365)	x_9	0	-0.387
	Layer-Specific Ozone	**$c_1(l)$**	**m(l)**
	Layer 6	35.66	37.96
	Layer 7	36.50	40.82
	Layer 8	37.42	43.09
	Layer 9	38.31	44.78
	Layer 10	39.20	46.08
	Layer 11	39.94	47.06
	Layer 12	40.62	47.93
	Layer 13	41.34	48.72
	Layer 14	42.27	50.03
	Layer 15	43.22	51.28
	Layer 16	44.14	51.49
	Layer 17	45.05	51.80
	Layer 18	45.96	53.47
	Layer 19	47.14	54.94
	Layer 20	48.55	55.10
	Layer 21	50.04	56.45
	Layer 22	51.62	57.49

$$p(l,d) = m(l) + b_1[x_1(l,d) - c_1(l)] + b_2[x_2(d) - c_2] + \cdots + b_9[x_9(d) - c_9]$$

In this case, the regression RMSE was 9.6 ppb from an unadjusted RMSE of 14.9 ppb. The regression R^2 was 33.4% from an unadjusted R^2 of 33%, a rather minor gain in model variance relative to the bias improvements.

2.4 Development of a Boundary Condition Adjustment Tool

The two regression models described above were codified into a portable and flexible Python-based tool that allows modelers to adjust their MOZART-based western ozone boundary conditions for regional domains that extend beyond the US west coast. Given that the regression model is formed from MOZART-THD comparisons over 2012-2016, we recommend against using the tool for dates well outside this analysis period. We carefully considered two options with respect to the adjustment approach: (1) apply the regression model results directly to gridded MOZART output ozone fields, which are then processed to regional model boundary condition files in the standard manner; (2) apply the regression model results to model-ready ozone boundary conditions derived from MOZART data. We decided that the latter approach is simpler and gives the user more flexibility to define which segments of specific boundaries to apply the adjustments. A disadvantage of this approach is that different regional models have unique boundary condition file formats. We elected to build the tool to adjust boundary conditions in CMAQ format to facilitate testing on the BAAQMD's modeling system. Later updates could be made to facilitate boundary conditions formats for other models.

The first step in tool development was to build simple text files containing the daily layer-specific ozone adjustment values from the regression models described above. We developed five separate annual files each listing 365 days per year; for cases where regional model boundary conditions spanning multiple years need to be adjusted (e.g., across New Year's Day), these files can be concatenated. This step alleviates the need for the user to apply the regression models themselves to derive the ozone adjustments.

The second step was to develop the boundary condition adjustment tool. We elected to base the tool on the Python scripting language, which allows the use of high-level libraries to read and manipulate netCDF files (the underlying format of CMAQ I/O) and perform mathematical functions. This minimizes code complexity and maximizes flexibility to easily adopt the tool to other model formats. Python is open-source free software and all Linux OS distributions come with basic Python libraries. Some additional libraries or specific library versions may need to be installed to support the tool; the tool requires the following:

- Python3
- xarray ≥ v0.10.6
- numpy ≥ v0.11

The tool replaces ozone concentrations in a CMAQ IO-API boundary conditions (BC) file with adjusted ozone profiles for a range of grid columns along a single boundary edge, from the surface to 5-6 km (depending on the vertical resolution of CMAQ). An additional input file defines the mapping between MOZART and CMAQ layers. Since the tool only modifies one BC edge at a time, the tool needs to be run sequentially for each edge to be modified; temporary intermediate BC files can be removed after the process. The ozone profiles used to replace CMAQ values enter from a comma-delimited text (CSV) file that contains the daily pre-calculated ozone adjustments described above.

After the Python scripts and supporting files have been copied and prerequisites installed on the system, follow these steps to run the tool:

1. Edit the CFG.json file
   - Edit the paths to input and output BC files
   - Edit the path to the layer mapping and ozone adjustment files
   - Set which side (W, N, E, S) and the range of boundary cells to adjust
2. Run the adjustment tool by typing the following at the Linux shell prompt:
   - > python run.py

The executable called “run.py” is a top-level script that opens and reads the configuration file, and then runs the adjustment tool script called “replace_cmaq_bcon.py”. A README file is provided with the Python tool that gives additional details on setup and usage.

The left scatterplots of Figure 9 compare unadjusted MOZART 10-cell ozone values against THD data on the days when THD data were available over the entire 2012-2016 period. Separate plots are shown for layers 1-5 (top) and layers 6-22 (bottom). The middle scatterplots compare adjusted ozone values against THD data on the same days; the adjusted data are taken from the daily regression model results contained in the Step 1 text file described above. The reduction in scatter is quite evident with the adjusted values, which shows a much narrower range relative to THD data. This is related to reducing the bias (differences in MOZART and THD mean ozone) but not reproducing the variability evident in the THD data.

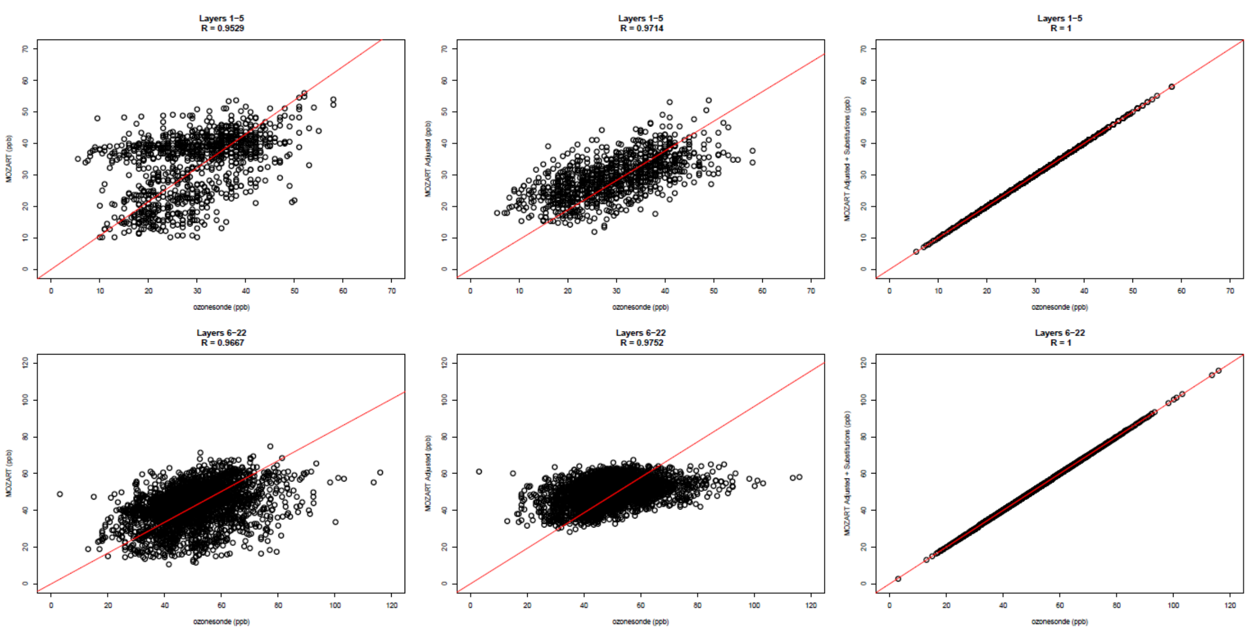

Figure 9. (Left) Scatterplots comparing unadjusted MOZART 10-cell ozone values against THD data on the days when THD data were available over the entire 2012-2016 period; MOZART layers 1-5 are shown in top row, layers 6-22 are shown in bottom row. (Middle) Scatterplots comparing adjusted ozone values against THD data on the same days. (Right) Scatterplots comparing ozonesonde substitution against THD data on the same days.

To include THD variability, we developed an alternative set of daily ozone profiles where THD data were directly substituted into the profiles on ozonesonde days, and also blended into the regression-based adjusted profiles on ozonesonde days ±1 and ±2 using weights of 2/3 and 1/3, respectively. This leaves roughly 1 day per week when only adjusted ozone from the regression model is used. Results on ozonesonde days are shown in the right scatterplots of Figure 9, which as a quality assurance step, verifies that the ozonesonde substitution replicates the original THD profiles. Figures 10 and 11 show comparisons of weighted ozonesonde adjustments/substitutions 1 and 2 days after ozonesonde days, respectively, against THD profiles on ozonesonde days. Additional improvements in variability are evident as the cloud of points align more closely along the 1:1 line on both days and for both sets of layer ranges. Similar patterns are seen on 1 and 2 days prior to ozonesonde days (not shown).

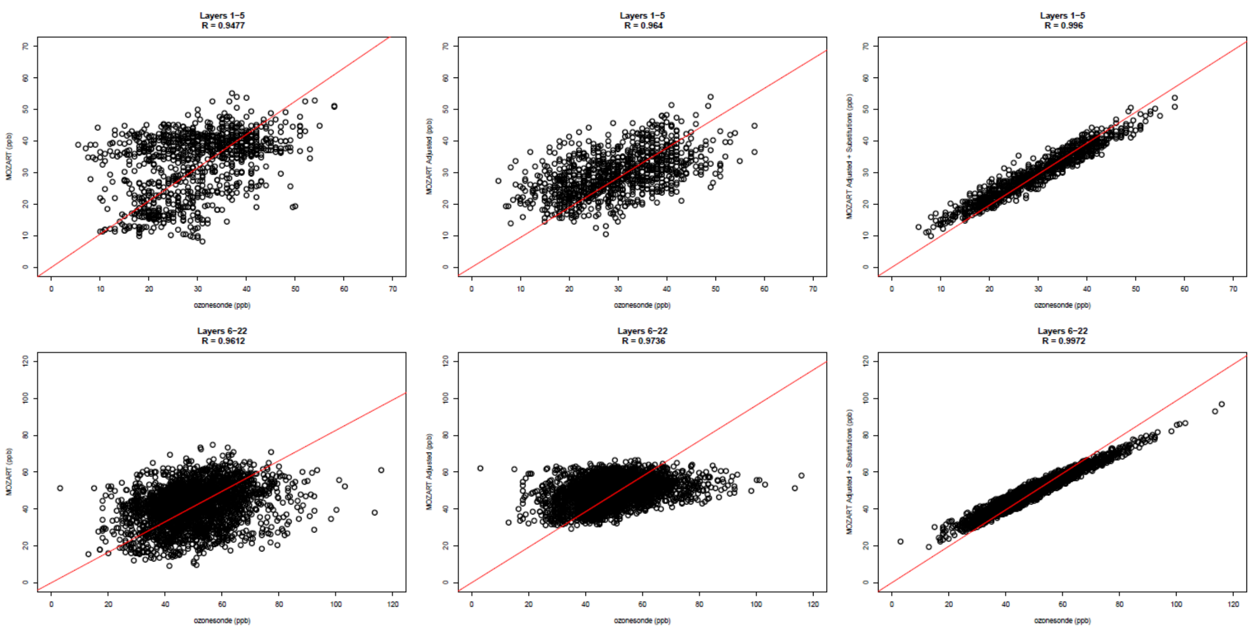

Figure 10. As in Figure 9, but for comparisons using ozone regression adjustments (middle) and hybrid regression adjustments/ozonesonde substitution (right) 1 day after THD ozonesonde days.

Figure 12 presents time-height cross sections of original MOZART 10-cell average ozone profiles in layers 1-22, the original adjusted ozone profiles from the regression model, and the final adjusted profiles with the hybrid THD ozonesonde substitution methodology described above. Each year is shown in sets of separate plots. The original adjustments from the regression model clearly alter the raw MOZART predictions as designed: reducing ozone in the lowest 5 layers while increasing ozone seasonally up to layer 22 (~5000 m). The hybrid ozonesonde substitution adds more temporal and spatial variability at all levels, and in fact increases upper-level ozone toward 100 ppb on certain ozonesonde days in the warm season. We attribute this feature to strong, deep subsidence in the climatologically persistent sub-tropical high pressure system that dominates weather patterns over the western US during these seasons.

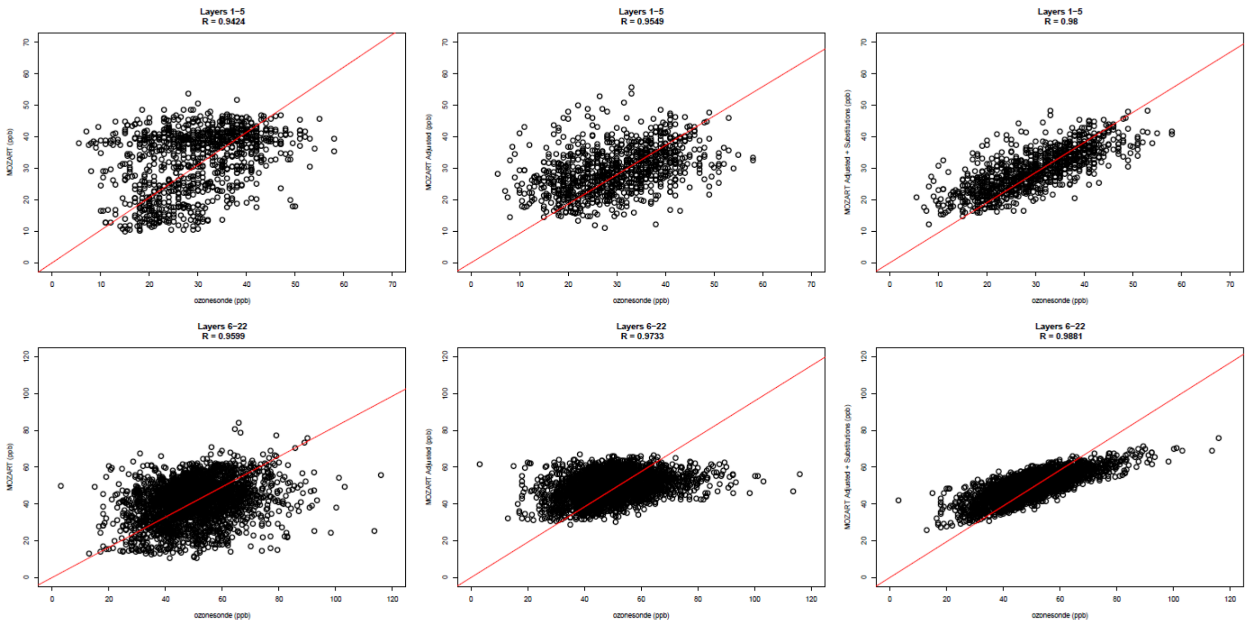

Figure 11. As in Figure 9, but for comparisons using ozone regression adjustments (middle) and hybrid regression adjustments/ozonesonde substitution (right) 2 days after THD ozonesonde days.

Based on these results, the hybrid regression model/ozonesonde substitution methodology was chosen as the final set of adjusted ozone profiles to be used with the BC adjustment tool. For initial testing and quality assurance checks, we applied the Python BC adjustment tool to a single CMAQ BC file (July 10, 2016) developed by the BAAQMD from MOZART data. Figure 13 shows curtain plots (vertical cross sections) of ozone on the western boundary from the original CMAQ file, the adjusted file (using the hybrid regression model/ozonesonde substitution profiles), and their differences. The adjusted ozone profile was applied to grid columns 92-185, representing the northern half of the western boundary. In this case, MOZART layer 22 extends into CMAQ layer 25 (~5500 m) based on our analysis of MOZART layer heights and CMAQ sigma layer structures. No adjustments above CMAQ layer 25 occurred. While impacts in the lowest 5 layers (~150 m) are minimal on this particular day, ozone increases up to 20 ppb occur in the northwest corner of the domain (rightmost edge of plot) in layers 17-24 (~1000-4000 m).

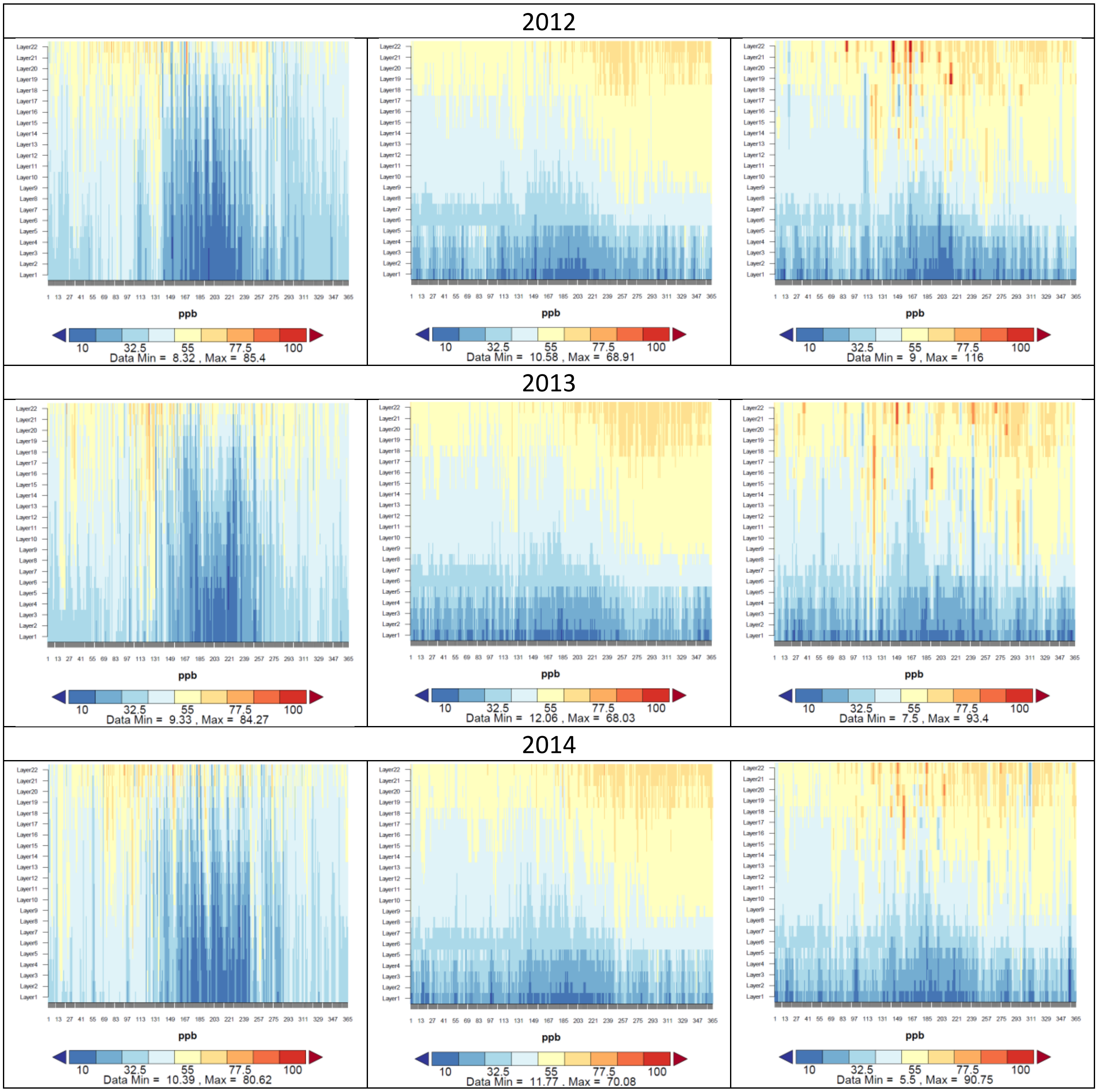

Figure 12. Time-height cross sections of original MOZART 10-cell average ozone profiles in layers 1-22 (left), adjusted ozone profiles from the regression model (middle), and final hybrid adjusted/substituted profiles (right) for each year between 2012 and 2014.

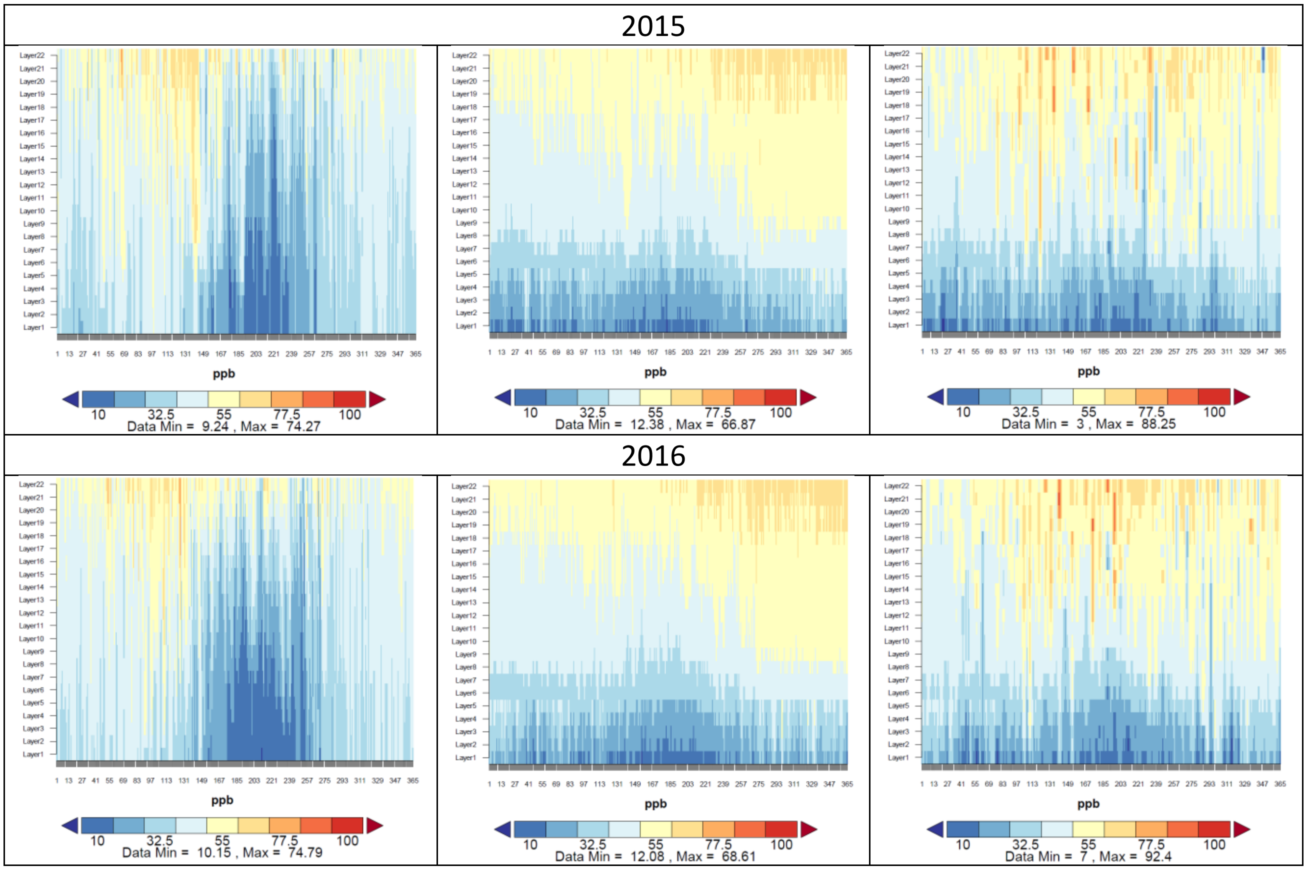

Figure 12 (continued). Time-height cross sections of original MOZART 10-cell average ozone profiles in layers 1-22 (left), adjusted ozone profiles from the regression model (middle), and final hybrid adjusted/substituted profiles (right) for each year between 2015 and 2016.

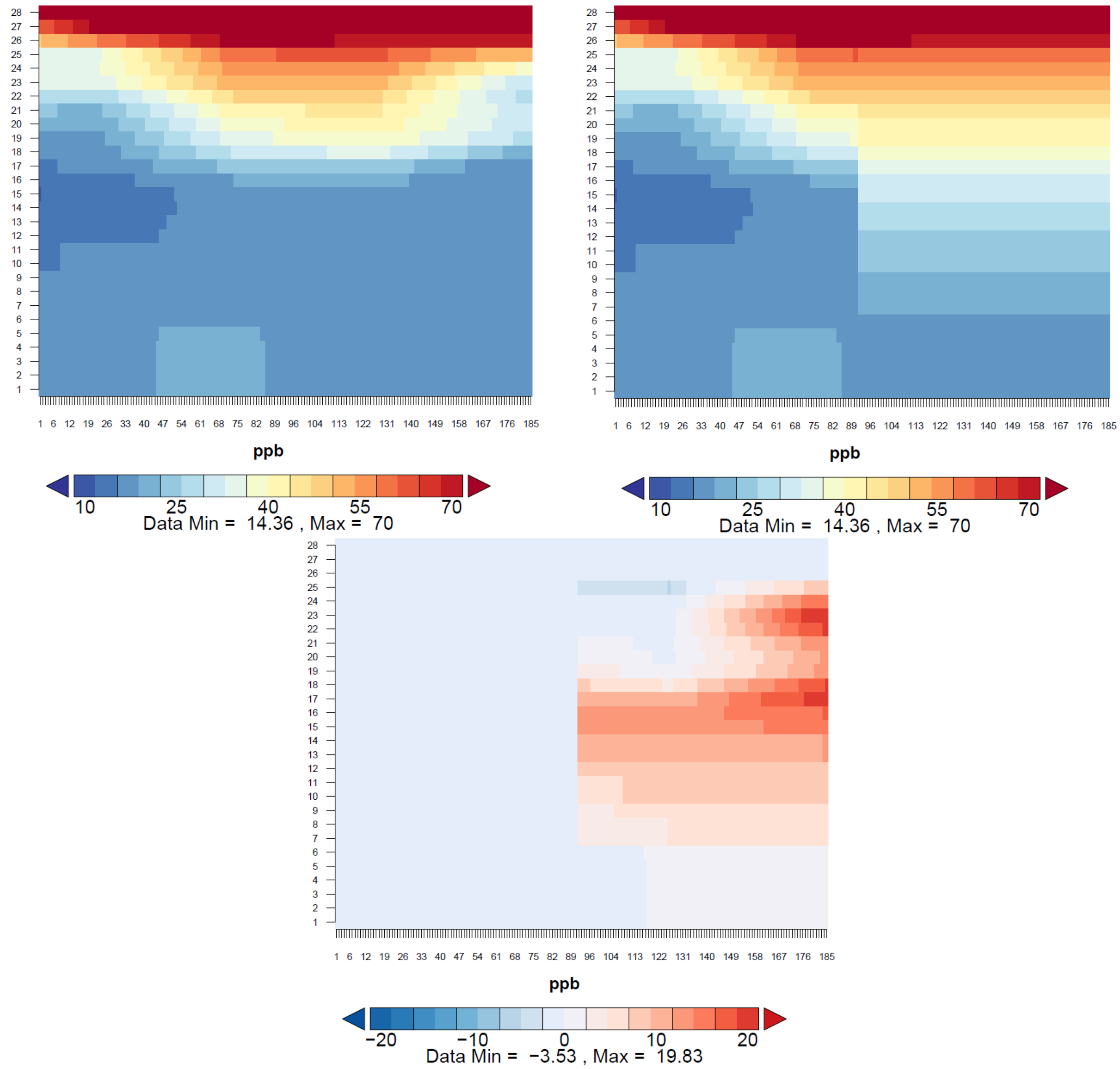

Figure 13. Curtain plots (vertical cross sections) of ozone on the western boundary of the BAAQMD CMAQ modeling domain (south is to the left, north is to the right), on July 10, 2016. (Top Left) Original CMAQ BC ozone; (Top Right) adjusted CMAQ BC ozone using the hybrid regression model/ozonesonde substitution profiles; (Bottom) differences between adjusted and original.

3.0 EVALUATION OF ADJUSTED CMAQ BOUNDARY CONDITIONS

3.1 Adjustment Configuration

The BAAQMD applied the Python-based BC adjustment tool to their 2016 daily CMAQ ozone boundary condition input files. The BAAQMD's modeling domain covers much of California and western Nevada (Figure 14), consisting of 185x185 grid cells with 4 km grid spacing and 28 vertical layers extending to an altitude of about 20 km (Table 3). As similarly described above, the BC adjustment tool was applied to grid columns 92-185 (northern half) of the western boundary; no other boundaries were modified. The MOZART-CMAQ layer mapping to receive ozone adjustments is shown in Table 3.

Table 3. Mapping of CMAQ layers to MOZART layers receiving ozone BC adjustments. CMAQ layers 26-28 were not modified.

CMAQ layer	CMAQ Height	Mozart Height	Mozart layer
1	25		1
2	52		1
3	81		1
4	112	118	1
5	144		2
6	180		2
7	218	235	2
8	258		3
9	302		3
10	348	354	3
11	398		4
12	450	475	4
13	507		5
14	566	600	5
15	692	727	6
16	827	856	7
17	974	989	8
18	1133	1123	9
19	1304	1260	10
20	1497	1540	12
21	1873	1977	14
22	2389	2488	16
23	3097	3028	18
24	4086	3902	20
25	5629	4871	22
26	8100	Not Adjusted	
27	12436		
28	19260		

The BAAQMD ran CMAQ over the year 2016 with and without adjusted ozone BCs and provided Ramboll with output concentrations files for further analysis and evaluation. Ramboll graphically and statistically compared CMAQ results over the ozone season (May-October) against 2016 CABOTS ozonesonde data and surface measurements at selected sites within the Bay Area and the Central Valley. Results are summarized in the sub-sections below.

3.2 Domain-Wide Maximum Impacts Over May-October

Figure 14 displays maximum (positive) and minimum (negative) hourly ozone impacts over the entire season resulting from the BC adjustment. These types of plots provide an initial characterization of impact patterns over the domain but are not representative of patterns for any specific hour or day. Hour/day-specific impacts are usually much smaller and exhibit a mix of positive and negative ozone differences confined to smaller areas of the domain, such as shown in the example for August 26 (Figure 15).

Figures 14 and 15 exemplify two basic paradigms in the adjusted BC impacts patterns:

- Positive ozone impacts typically originate from increased BCs aloft (MOZART layers 6-22, CMAQ layers 15-25, 600-5000 m), which mix down during the day over high-elevation topography at increments that can exceed 20 ppb, then disperse at the surface to other area of the domain;

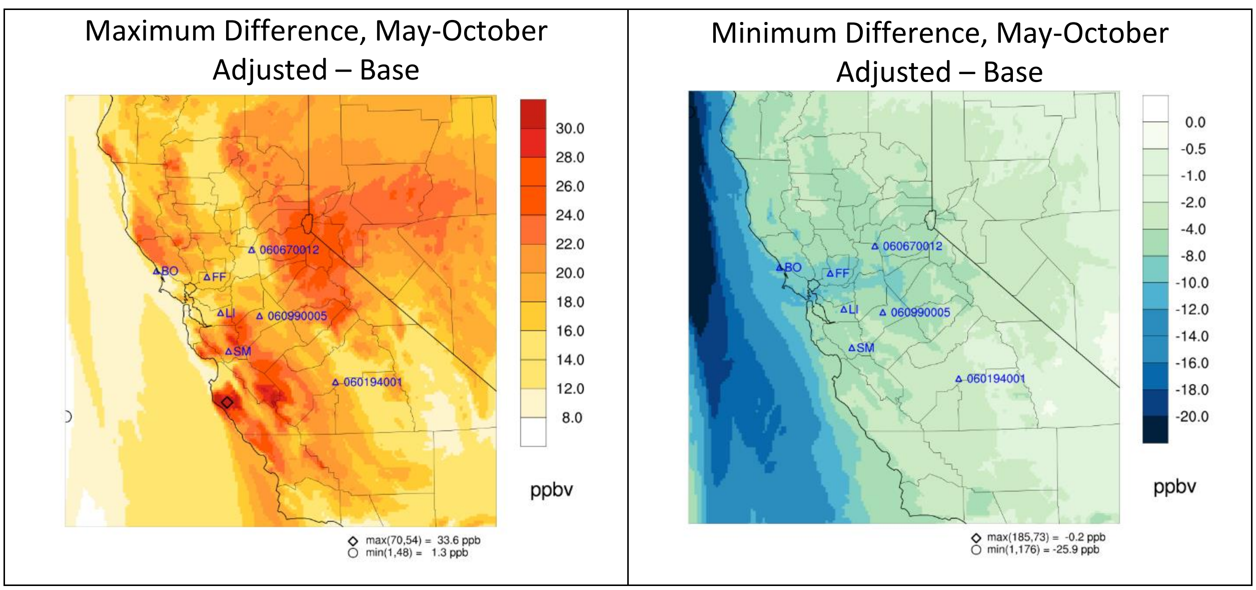

Figure 14. Maximum (left) and minimum (right) hourly ozone differences between the adjusted and unadjusted BC simulations over May-October, 2016. Note that each plot does not represent results for a single day; difference values in each grid cell may occur at different hours and dates.

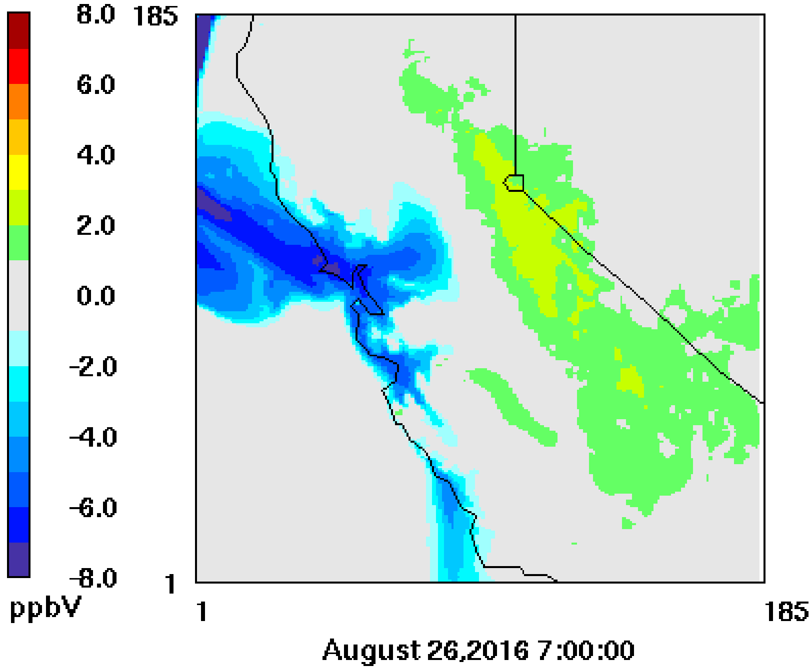

Figure 15. Example of 1-hour ozone difference between the adjusted and unadjusted BC simulations at 7 AM UTC (midnight local daylight time), August 26, 2016.

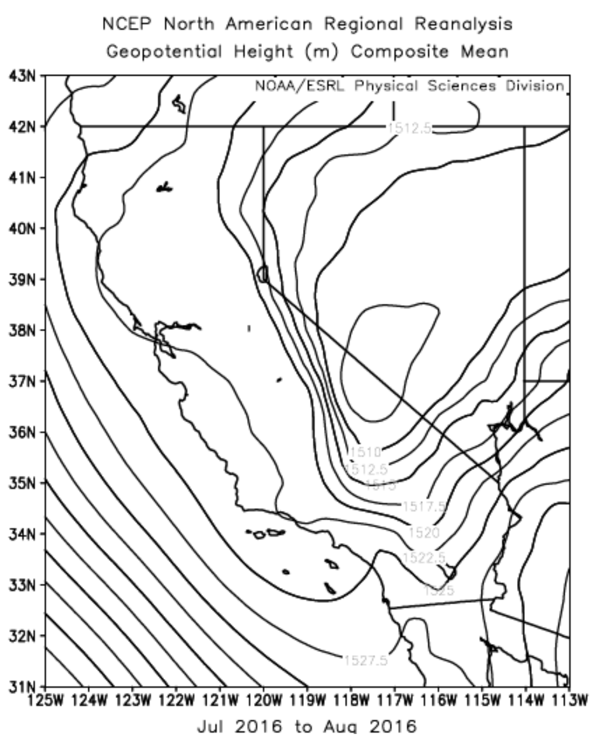

Figure 16. July-August 2016 mean 850 mb geopotential heights (m) over California and Nevada. Winds at this level are proportional and parallel to the height contour gradient, which show consistently strong northwesterly flow along the California coastline and lighter winds over the Central Valley (UC Davis, 2018).

- Negative ozone impacts typically originate from reduced BCs in the marine boundary layer (MOZART layers 1-5, CMAQ layers 1-14, 0-600 m), where increments greater than 10 ppb are maintained in the stable environment while transported along the coastline in the consistent northwesterly flow (Figure 16), and then occasionally drawn through coastal topographic gaps such as the Bay Area. Once onshore, these increments are vertically mixed within the daytime boundary layer, leading to negligible to small daytime impacts.

3.3 Comparisons Against CABOTS Ozonesondes

CABOTS operated two coastal ozonesonde launch sites at Bodega Bay (BB) and Half Moon Bay (HMB). The BB site is located on the Sonoma County coastline northwest of the Bay Area and most often represents an upwind source of air entering the northern Bay Area from the Pacific Ocean. BB was operated from mid-May through mid-August with launches nearly every day. The HMB site is located on the San Mateo County coastline just west of the central Bay Area and represents an upwind source of air entering the southern Bay Area from the Pacific Ocean, yet sometimes measures ozone generated in the Bay Area and the Central Valley during episodes of offshore flow. The HMB site was operated for a single month (mid-July through mid-August).

Figure 17 compares monthly observed ozone profile distributions at BB to CMAQ simulations with unadjusted and adjusted BCs. Individual ozone measurements throughout each daily profile were averaged to each CMAQ layer to facilitate a consistent comparison (note that not all CMAQ layers contain ozone measurements). Simulated ozone profiles were taken from the hour during which the ozonesonde was launched. Each of the monthly plots in Figure 17 show consistent features. Near the surface (layers 1-13), CMAQ overpredicted ozone, especially later in the period, with negligible to little effect from the BC adjustment. The overprediction bias of ~5 ppb may be related to insufficient ozone destruction from reactions with oceanic halogens in the SAPRC07 chemical mechanism. Above the marine boundary layer (layers 15-25), the unadjusted CMAQ simulation tended to underpredict ozone by 10 ppb or more during June-August, while the adjusted simulation reduced that bias markedly, at least for median ozone (note the much smaller inter-quartile ranges and whiskers). In May, however, the unadjusted CMAQ profile was fairly un-biased aloft and the BC adjustment contributed toward a small overprediction bias.

A more detailed analysis of the ozone comparisons at BB are shown in the scatter plots in Figure 18 and 19 and the statistical summaries in Tables 4 and 5. These analyses group model-measurement comparisons into two height ranges: layers 1-14 and layers 15-25 (note that CMAQ layer 14 did not include ozone measurements). The overprediction bias in the lower layers (Figure 18) is clear for the latter three months, and while the BC adjustment shows a small positive increase in ozone, it is not sufficient to alter the linear regression fit through the data in any month. This is also shown in the statistics (Table 4), which indicate very little change in regression and minor impacts on the coefficient of determination (R^2, the square of correlation). In layers aloft (Figure 19), the model largely underpredicts high ozone but performs well for lower ozone. However, the higher ozone introduced with the BC adjustment

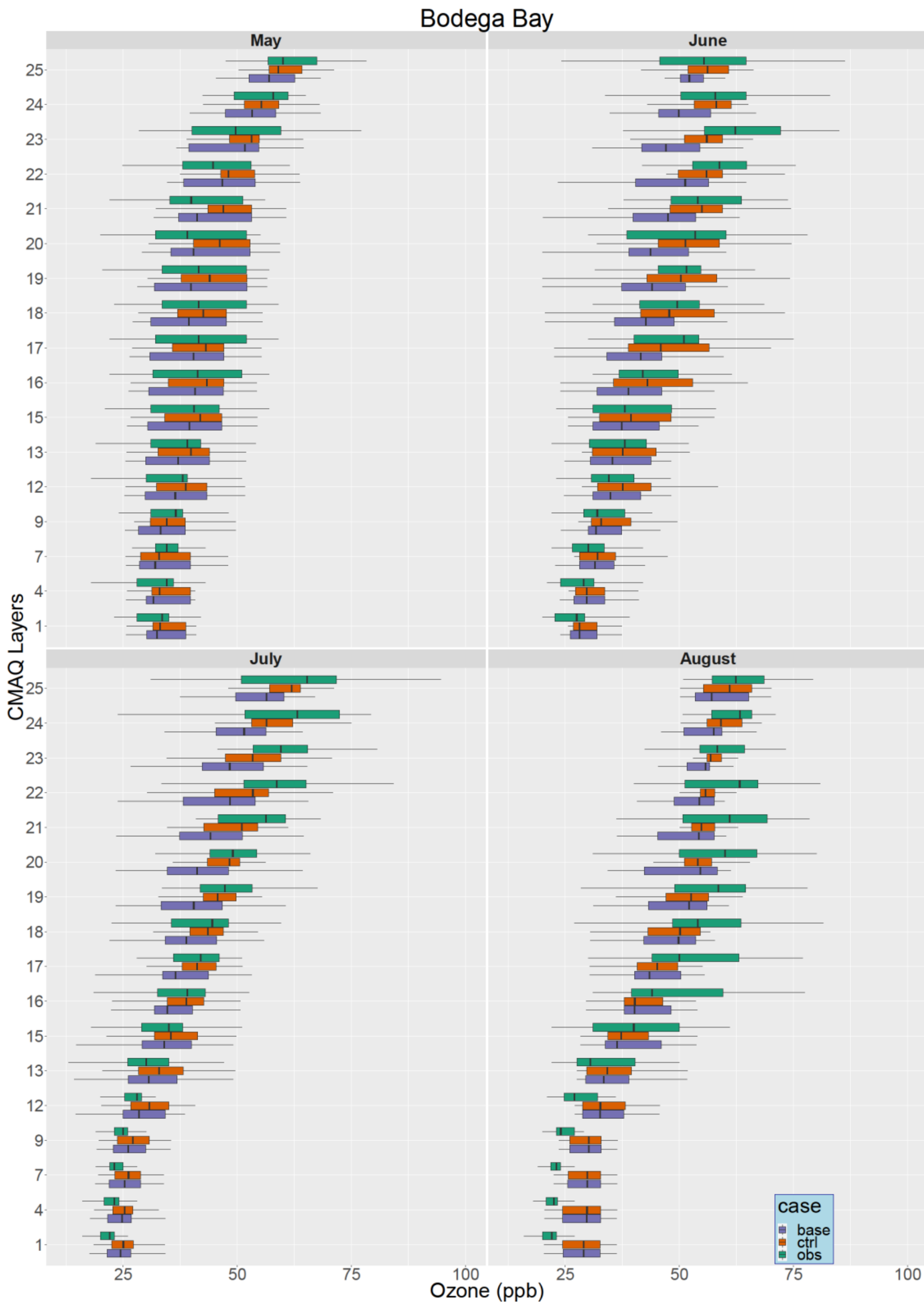

Figure 17. Comparison of monthly ozone profile distributions at Bodega Bay: observations (green), CMAQ with unadjusted BCs (blue) and CMAQ with adjusted BCs (orange). Boxes represent inter-quartile ranges, vertical lines represent medians, and whiskers represent ±1.5 times the inter-quartile range. Extreme outliers are not plotted.

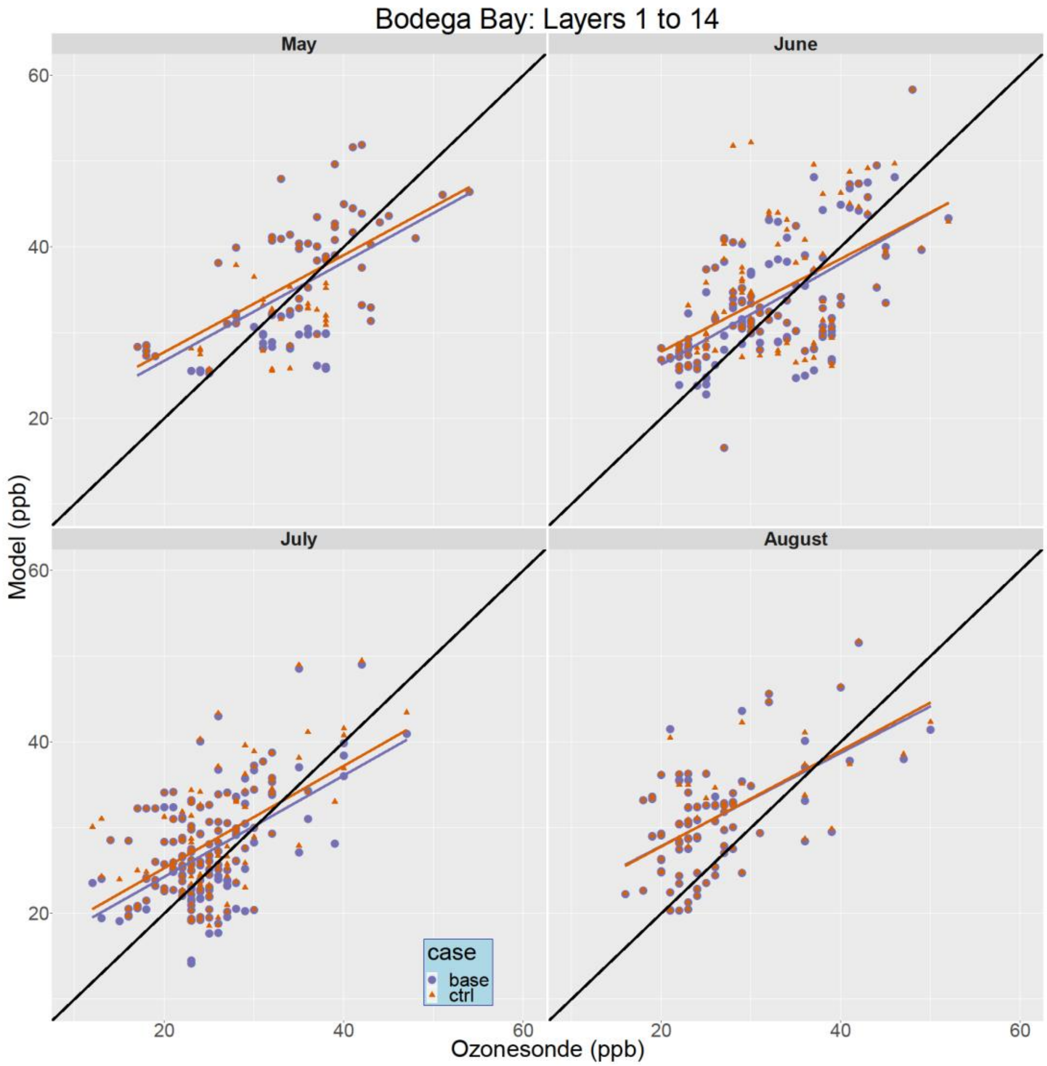

Figure 18. Scatter plots of CMAQ simulated ozone (unadjusted BC as blue circles, adjusted BC as red triangles) versus ozonesonde measurements at Bodega Bay by month and collectively over CMAQ layers 1-14 (0-600 m). Linear regression lines are shown for both sets of CMAQ data; the 1:1 line is shown in black.

Table 4. Linear regression statistics by month from Figure 18.

Month	Case	Slope	Intercept	R^2
May	Unadjusted	0.574	15.2	0.37
	Adjusted	0.566	16.4	0.42
June	Unadjusted	0.590	14.4	0.36
	Adjusted	0.541	16.9	0.28
July	Unadjusted	0.591	12.4	0.27
	Adjusted	0.596	13.3	0.29
August	Unadjusted	0.543	16.9	0.30
	Adjusted	0.560	16.6	0.32

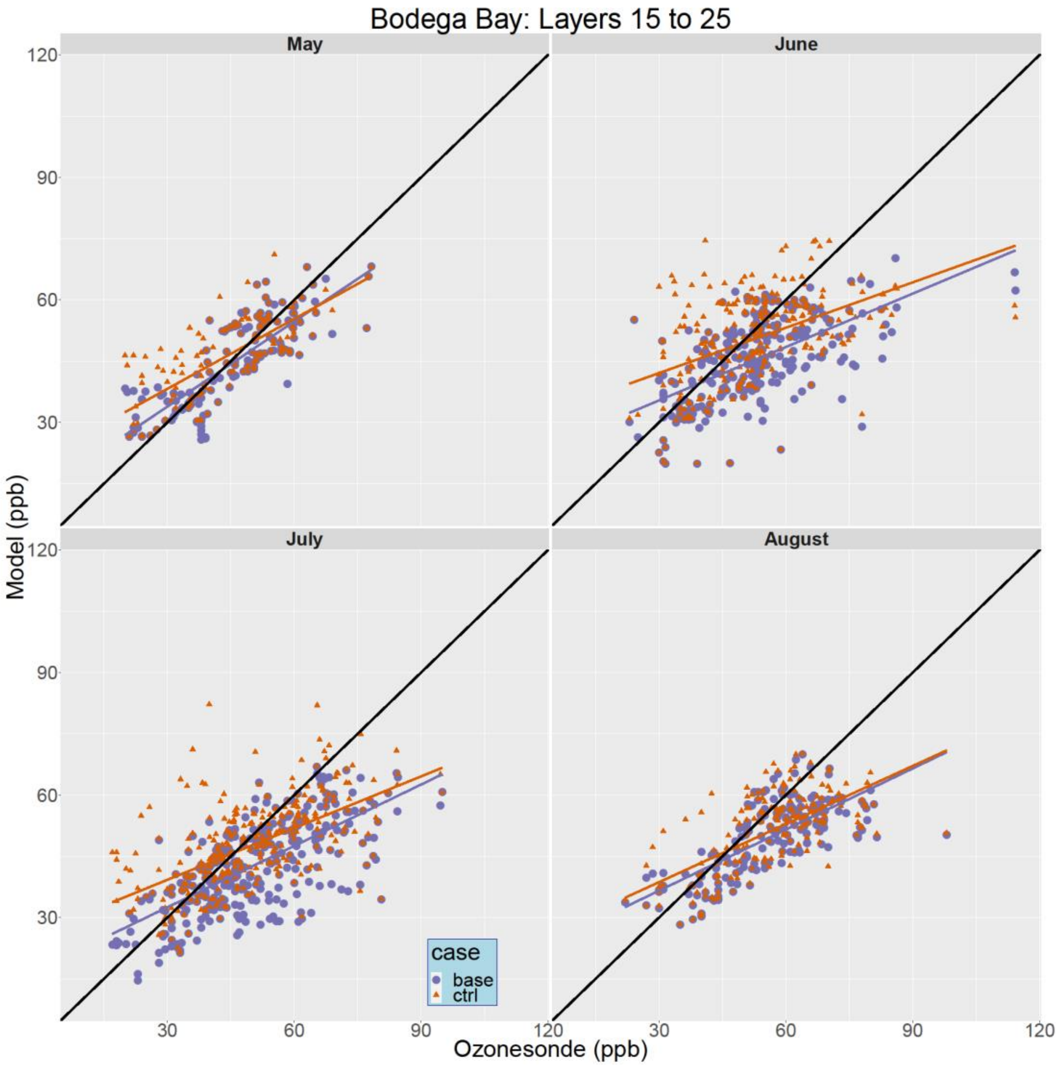

Figure 19. Scatter plots of CMAQ simulated ozone (unadjusted BC as blue circles, adjusted BC as red triangles) versus ozonesonde measurements at Bodega Bay by month and collectively over CMAQ layers 15-25 (600-5000 m). Linear regression lines are shown for both sets of CMAQ data; the 1:1 line is shown in black.

Table 5. Linear regression statistics by month from Figure 19.

Month	Case	Slope	Intercept	R^2
May	Unadjusted	0.695	13.0	0.66
	Adjusted	0.571	21.0	0.53
June	Unadjusted	0.436	22.3	0.36
	Adjusted	0.370	30.9	0.22
July	Unadjusted	0.501	17.4	0.47
	Adjusted	0.422	26.5	0.35
August	Unadjusted	0.499	21.6	0.50
	Adjusted	0.474	24.4	0.42

tends to increase only low- to mid-range ozone near the median, which slightly degrades statistical metrics each month by reducing the regression slope and R^2. This is consistent with the improved median ozone, but much smaller inter-quartile ranges visually evident in the profile plots of Figure 17; it is also consistent with the effort to reduce the bias in MOZART-derived BCs toward less-variable observed seasonal means.

Figure 20 compares observed ozone profile distributions at HMB to CMAQ simulations with unadjusted and adjusted BCs for the July-August measurement period. Features are consistent with the BB analysis: (1) near-surface overpredictions of ~10 ppb and no significant impact from the BC adjustment; (2) some improvement in the smaller ozone underpredictions aloft with the adjusted BCs, but to a much lesser extend seen at BB and a similar lack of improvement at the highest observed ozone concentration ranges. Observed and simulated ozone at lower elevations at this site may be influenced more often by Bay Area and Central Valley influences during occasional offshore flow regimes.

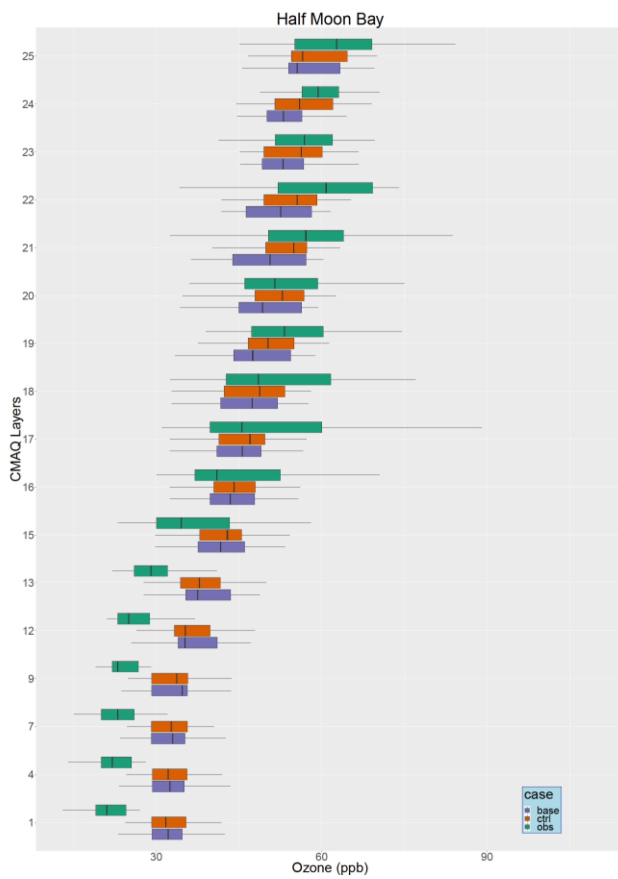

Figure 20. Comparison of July-August ozone profile distributions at Half Moon Bay: observations (green), CMAQ with unadjusted BCs (blue) and CMAQ with adjusted BCs (orange). Boxes represent inter-quartile ranges, vertical lines represent medians, and whiskers represent ±1.5 times the inter-quartile range. Extreme outliers are not plotted.

Figure 21 shows scatter plots at HMB arranged similarly for lower layers (1-14) and higher layers (15-25); regression statistics are presented in Table 6. There is very little difference in statistical performance between the unadjusted and adjusted CMAQ simulation results, however similar effects occur as seen at BB. Overall, this site appears to be less influenced by the choice of ozone BCs than the more northern BB site. Again, this may be caused by a somewhat stronger local influence from the Bay Area and/or more influence from unadjusted portions of the western boundary.

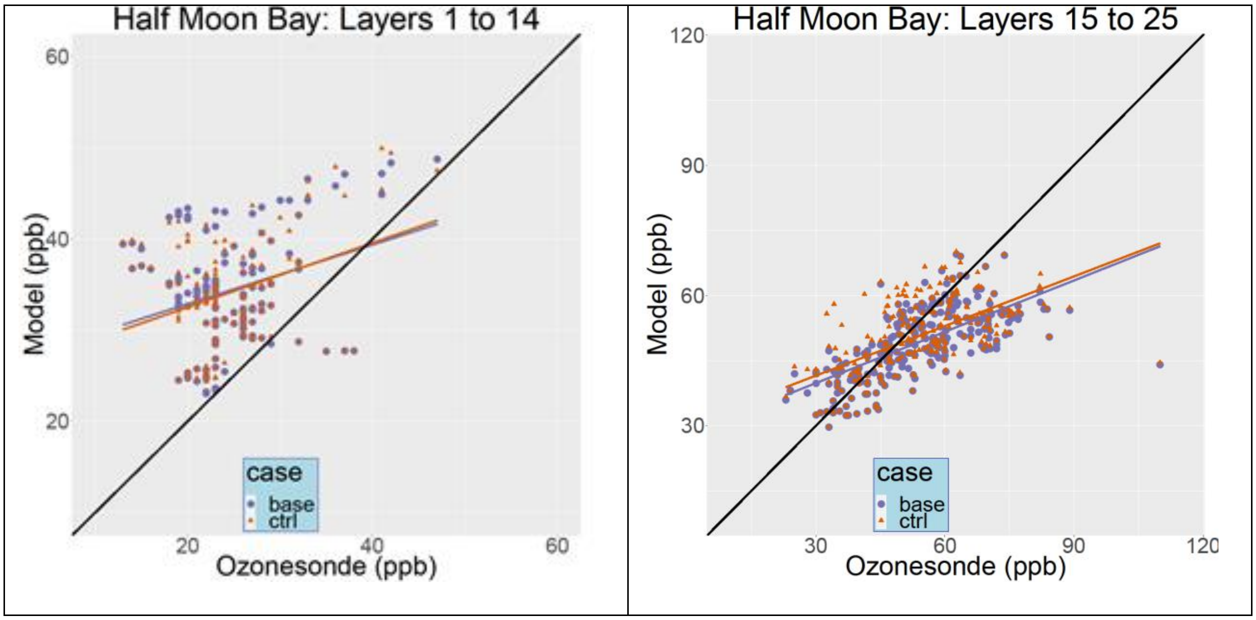

Figure 21. Scatter plots of CMAQ simulated ozone (unadjusted BC as blue circles, adjusted BC as red triangles) versus ozonesonde measurements at Half Moon Bay collectively over CMAQ layers 1-14 (0-600 m, left) and 15-25 (600-5000 m, right). Linear regression lines are shown for both sets of CMAQ data; the 1:1 line is shown in black.

Table 6. Linear regression statistics by month from Figure 21.

Layers 1 to 14

Month	Case	Slope	Intercept	R^2
Jul-Aug	Unadjusted	0.325	26.3	0.09
	Adjusted	0.352	25.4	0.11

Layers 15 to 25

Month	Case	Slope	Intercept	R^2
Jul-Aug	Unadjusted	0.394	27.9	0.44
	Adjusted	0.381	30.1	0.36

3.4 Ozone Impacts at Surface Monitoring Sites

Simulated ozone impacts from the BC adjustments were evaluated at key monitoring sites around the Bay Area and in the Central Valley. In the Bay Area, we selected the upwind site at Bodega Bay (BO), a northern inland site at Fairfield (FF), and eastern and southern sites commonly measuring the highest ozone in the Bay Area: Livermore (LI) and San Martin (SM). In the Central Valley, we selected three sites: Folsom to the east of Sacramento; Modesto in the north-central San Joaquin Valley, and Parlier near Fresno.

Figure 22 displays time series of hourly simulated and observed ozone over the month of June at the four Bay Area sites. In all cases, the effects of the ozone BC adjustment are rather small and difficult to differentiate except for a few scattered days. The largest noticeable effects are: (1) an occasional increase in morning minimum ozone; (2) some positive and negative impacts to daily maximum ozone. Arguably there are more evident impacts at the inland and southern Bay Area sites with more positive increments than negative. Our review of all other months during the ozone season exhibit very similar impacts (not shown), so June is considered a reasonably representative example.

To statistically evaluate impacts over the entire ozone season (May-October), Figure 23 displays scatter plots of 1-hour ozone at these same four sites. Statistics shown in each plot are calculated for all 1-hour observation-prediction pairings with no concentration cutoff (i.e., no observation floor such as 60 ppb) so that performance impacts from adjusted BCs can be assessed over the full ozone range. Except for Bodega Bay, ozone is adequately simulated with a tendency for overprediction. Despite calculating statistics with no cutoff, the model performs generally well in the base (unadjusted) case over this period, with $R^2 > 0.6$, overprediction bias ≤15%, and gross error ≤25% among three of the four sites (Emery et al., 2016). The adjusted ozone BC simulation slightly raises ozone, thereby raising the overprediction bias and gross error by a few percentage points, especially at the inland sites. Overall, however, there is no significant change in model performance statistics or CMAQ's characterization of hourly ozone with the ozone BC adjustment.

Figure 24 displays time series of hourly simulated and observed ozone over the month of June at the three Central Valley sites. Like the inland Bay Area sites at FF, LI and SM, similarly small impacts are evident at these sites. Most of the effects from the ozone BC adjustment tend toward small increases in both minimum and maximum daily ozone on a few scattered days. June a reasonably representative example of other months in the seasons (not shown).

Figure 25 displays scatter plots of 1-hour ozone at these three sites over the entirety of the May-October season. Ozone is well-simulated at these sites with a slight tendency toward underprediction: $R^2 > 0.75$, underprediction bias ≤15%, and gross error ≤25%. Like the Bay Area, the adjusted ozone BC simulation slightly raises ozone, thereby improving the underprediction bias by a few percentage points. Overall, however, there is no significant change in model performance statistics or CMAQ's characterization of hourly ozone with the ozone BC adjustment.

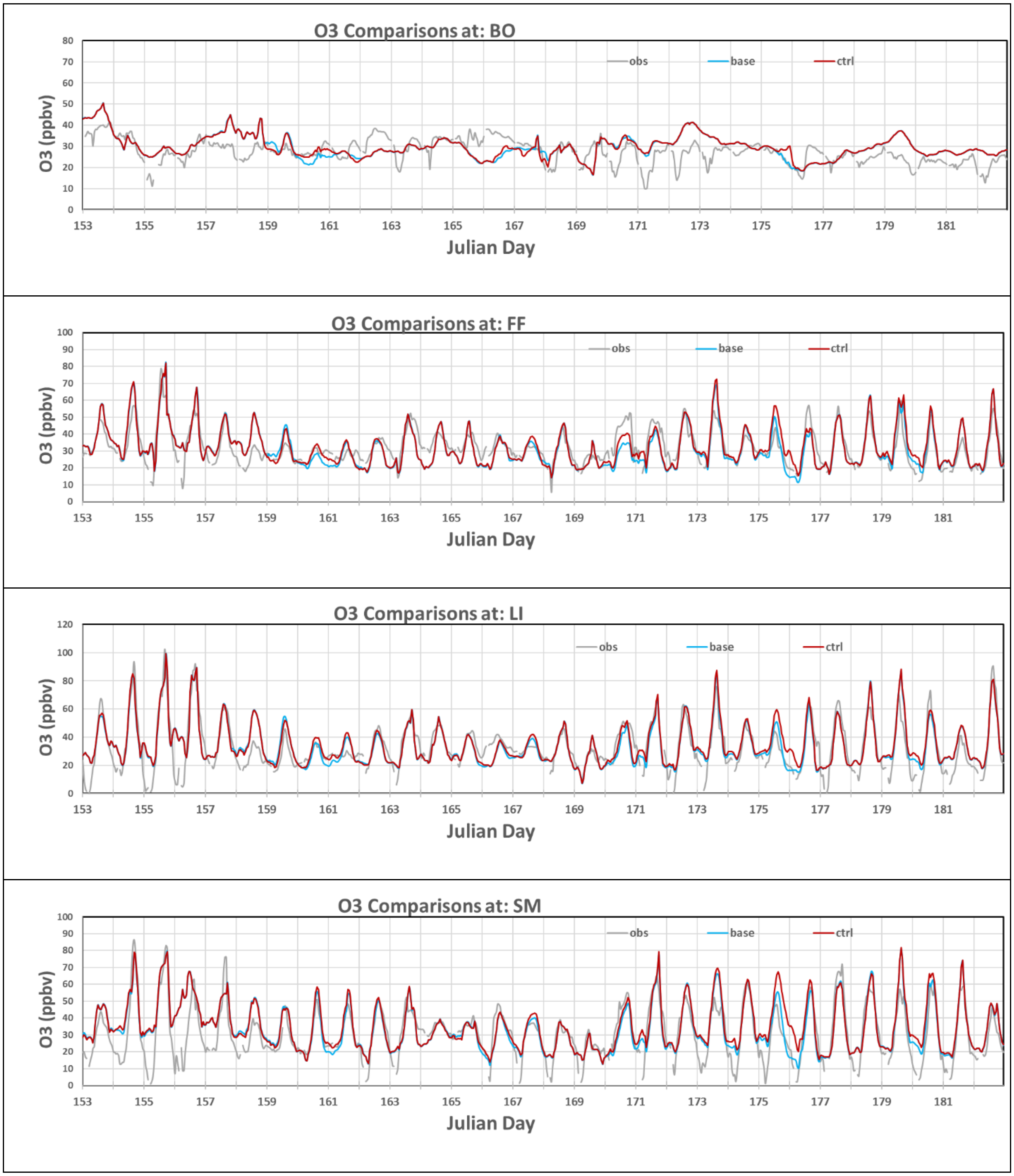

Figure 22. Time series of 1-hour ozone over June 2016 at four Bay Area sites: Bodega Bay (BO, top), Fairfield (FF, second from top), Livermore (LI, third from top), and San Martin (SM, bottom). Observations are in grey, CMAQ simulation with unadjusted ozone BCs is in blue, and CMAQ simulation with adjusted ozone BCs is in red.

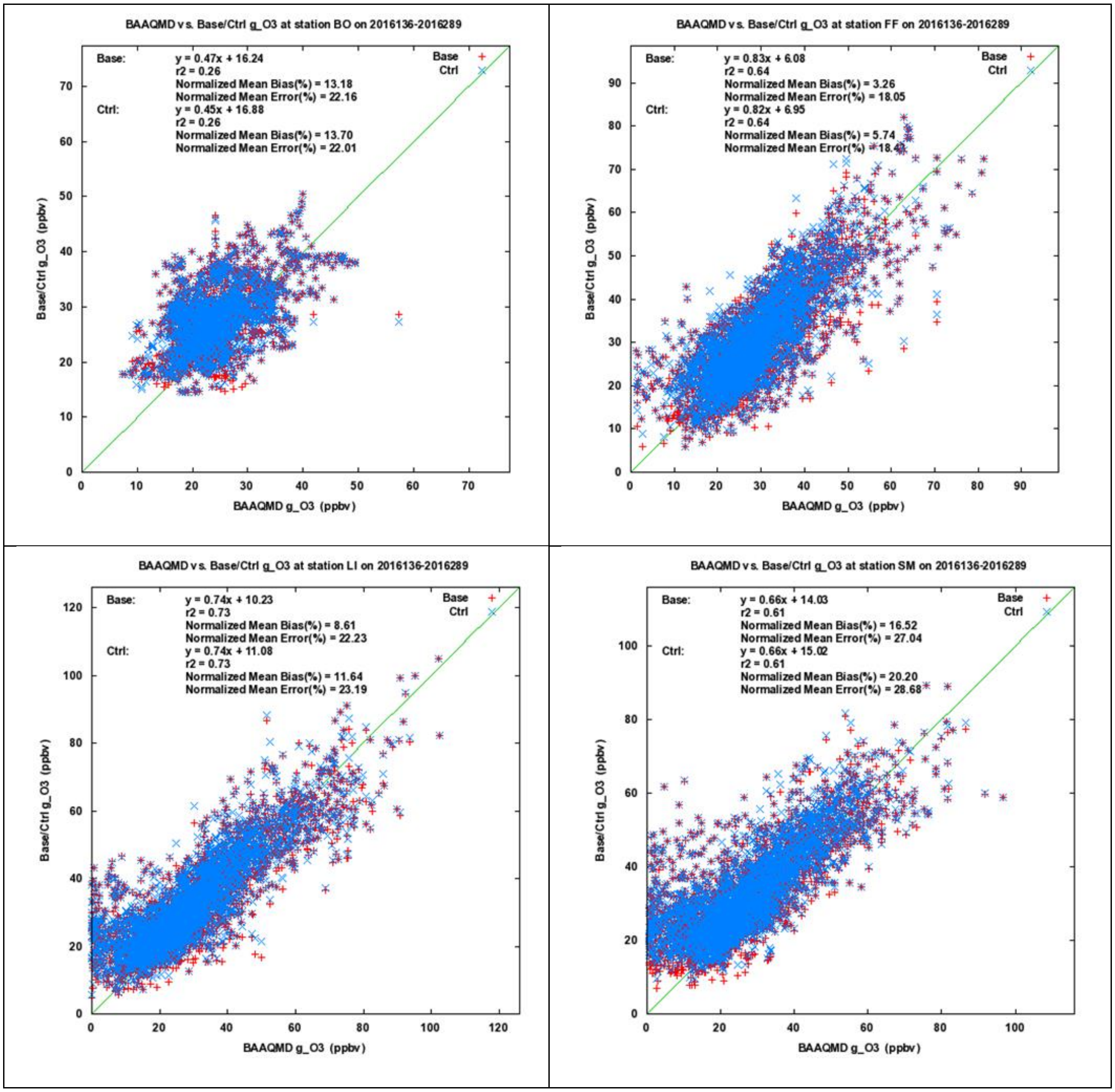

Figure 23. Scatter plots of 1-hour ozone over May-October 2016 at four Bay Area sites: Bodega Bay (BO, top left), Fairfield (FF, top right), Livermore (LI, bottom left), and San Martin (SM, bottom right). CMAQ simulation with unadjusted ozone BCs is in red, and CMAQ simulation with adjusted ozone BCs is in blue. Statistics are calculated for all 1-hour observation-prediction pairings with no concentration cutoff (no floor).

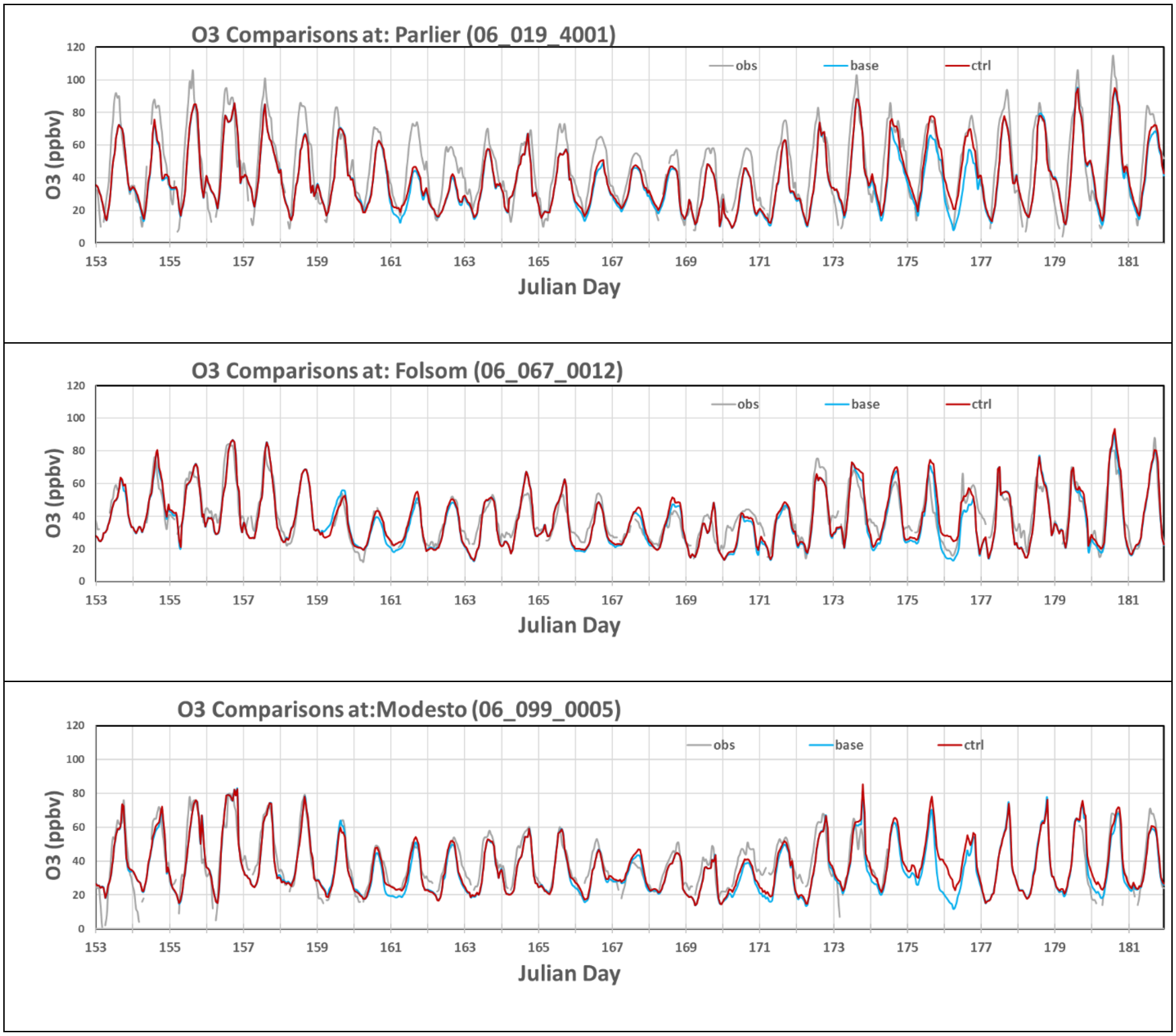

Figure 24. Time series of 1-hour ozone over June 2016 at three Central Valley sites: Parlier (top), Folsom (middle), and Modesto (bottom). Observations are in grey, CMAQ simulation with unadjusted ozone BCs is in blue, and CMAQ simulation with adjusted ozone BCs is in red.

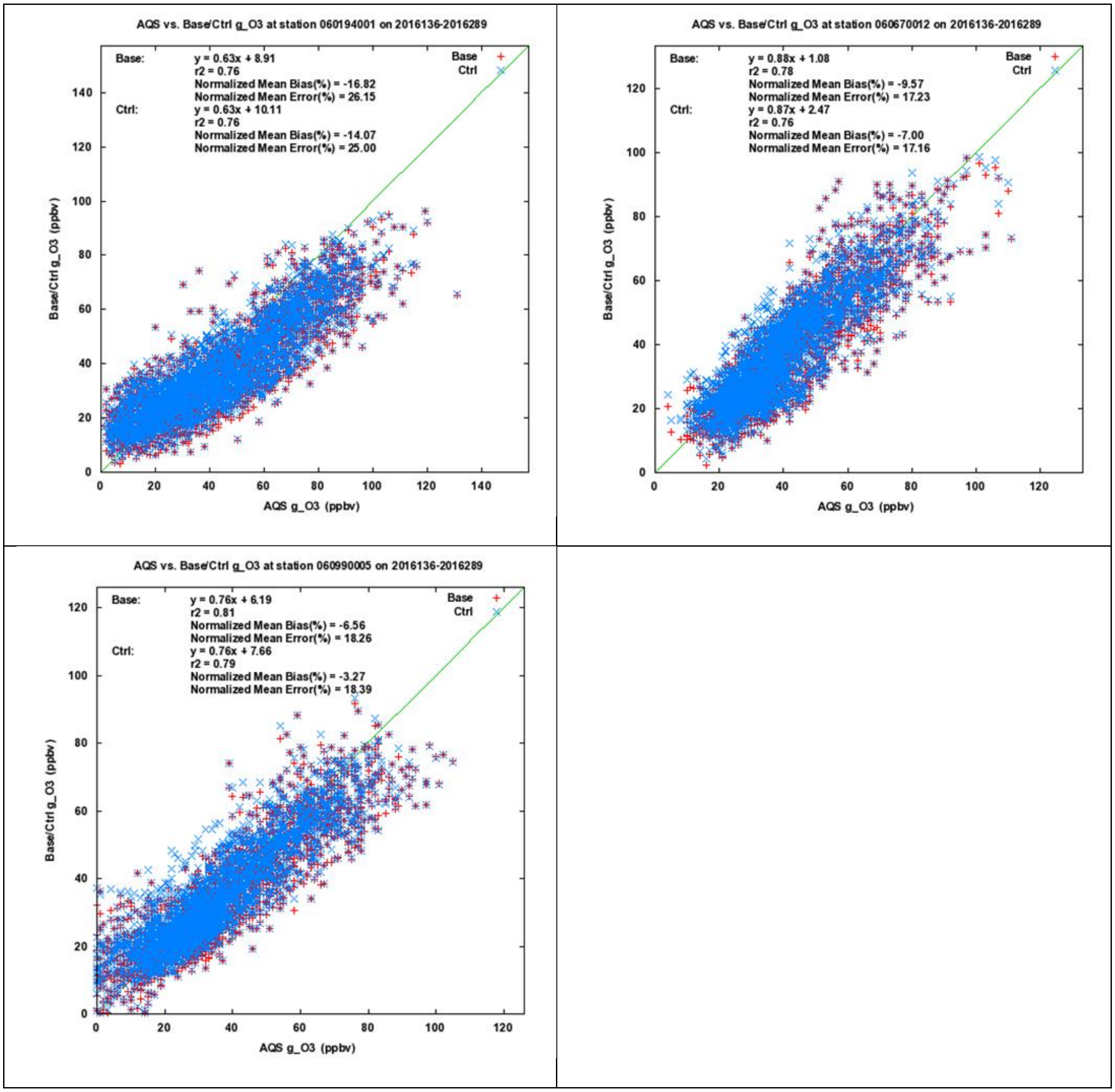

Figure 25. Scatter plots of 1-hour ozone over May-October 2016 at three Central Valley sites: Parlier (top left), Folsom (top right), and Modesto (bottom left). CMAQ simulation with unadjusted ozone BCs is in red, and CMAQ simulation with adjusted ozone BCs is in blue. Statistics are calculated for all 1-hour observation-prediction pairings with no concentration cutoff (no floor).

3.5 Alternative Adjustment Test

Given the limited ozone response resulting from the initial BC adjustment, an alternative BC adjustment was tested. In this case, the adjustment was extended to cover grid columns 60-185 (northern two-thirds) of the western boundary, and grid columns 1-60 (western third) of the northern boundary. The vertical layer mapping remained consistent with the initial case.

Comparisons to CABOTS ozonesondes are presented in Figures 26-30 and Tables 7-9. At BB, the alternative BC case results in larger ozone impacts within the marine boundary layer (CMAQ layers 1-14), most significantly in May and July (other months at BB, as well as HMB, exhibit similarly small effects as the initial adjustment). In May, the alternative BC case reduces marine layer ozone, leading to worse agreement with ozonesonde data than the unadjusted case. Scatter plots of these comparisons show a flatter slope and significantly worse R^2 value. In July, the alternative BC case indicates slight improvements within the marine boundary layer relative to the unadjusted case, with improved regression slope and R^2. Like the initial adjustment, this case results in systematically higher ozone in aloft layers 15-25 in all months at both BB and HMB, and much smaller variability according to inter- and extra-quartile ranges than the observations in all months and at all levels.

Similarly minor ozone effects occur in the alternative BC case at all surface monitoring sites within the Bay Area and Central Valley, except for Bodega Bay, where the overprediction bias over the entire ozone season is markedly improved. However, as seen in the BB ozonesonde results, overall model-observation correlation at Bodega Bay is reduced and the regression slope is flattened as a result of the model's lack of variability. At other Bay Area monitoring sites, the increase in seasonal overprediction bias is slightly worse than the initial BC adjustment case, while at Central Valley sites, the improvement in seasonal underprediction bias is slightly better. Overall, there is again no significant performance impact from these alternative BC adjustments.

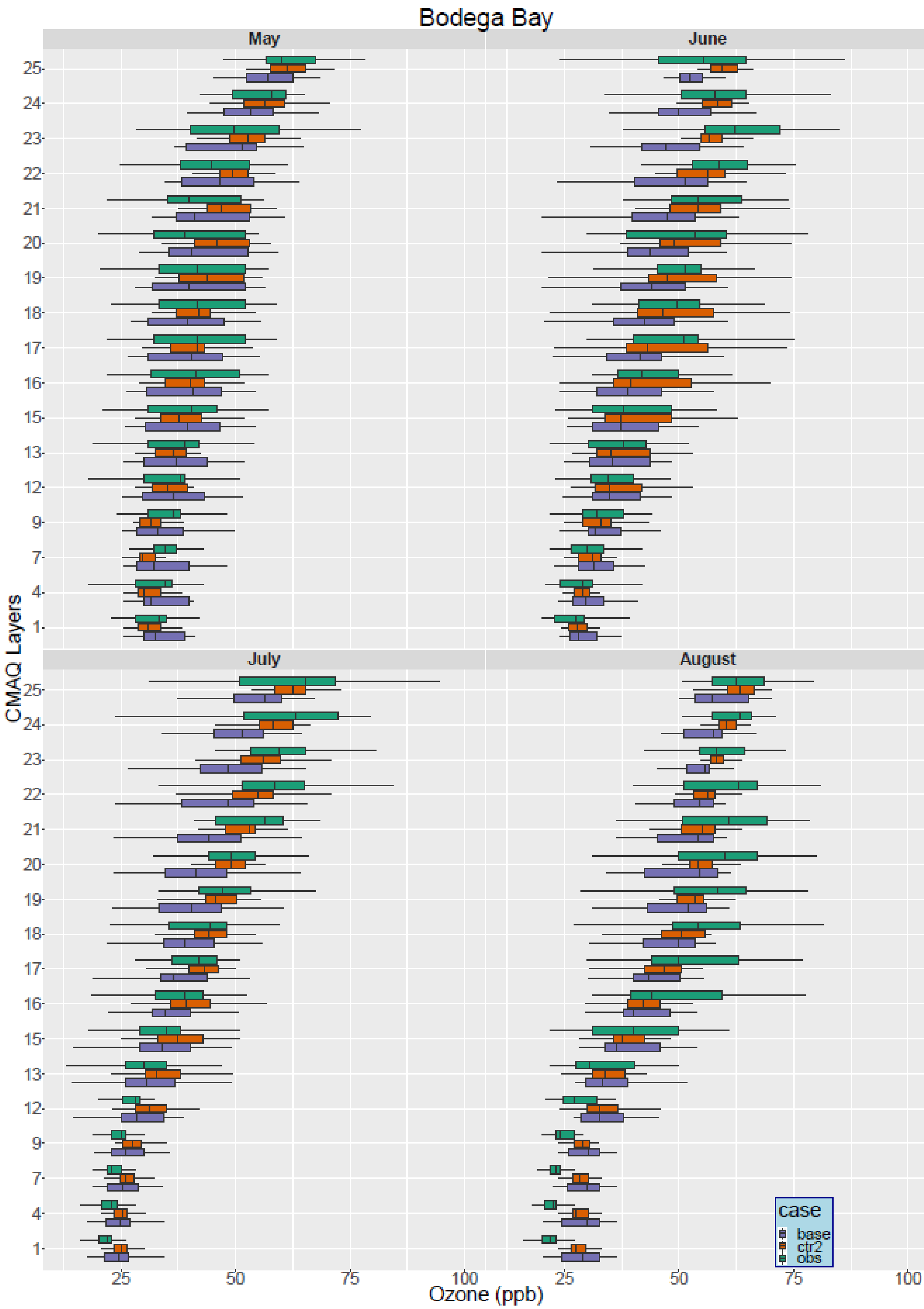

Figure 26. Comparison of monthly ozone profile distributions at Bodega Bay: observations (green), CMAQ with unadjusted BCs (blue) and CMAQ with alternative adjusted BCs (orange). Boxes represent inter-quartile ranges, vertical lines represent medians, and whiskers represent ±1.5 times the inter-quartile range. Extreme outliers are not plotted.

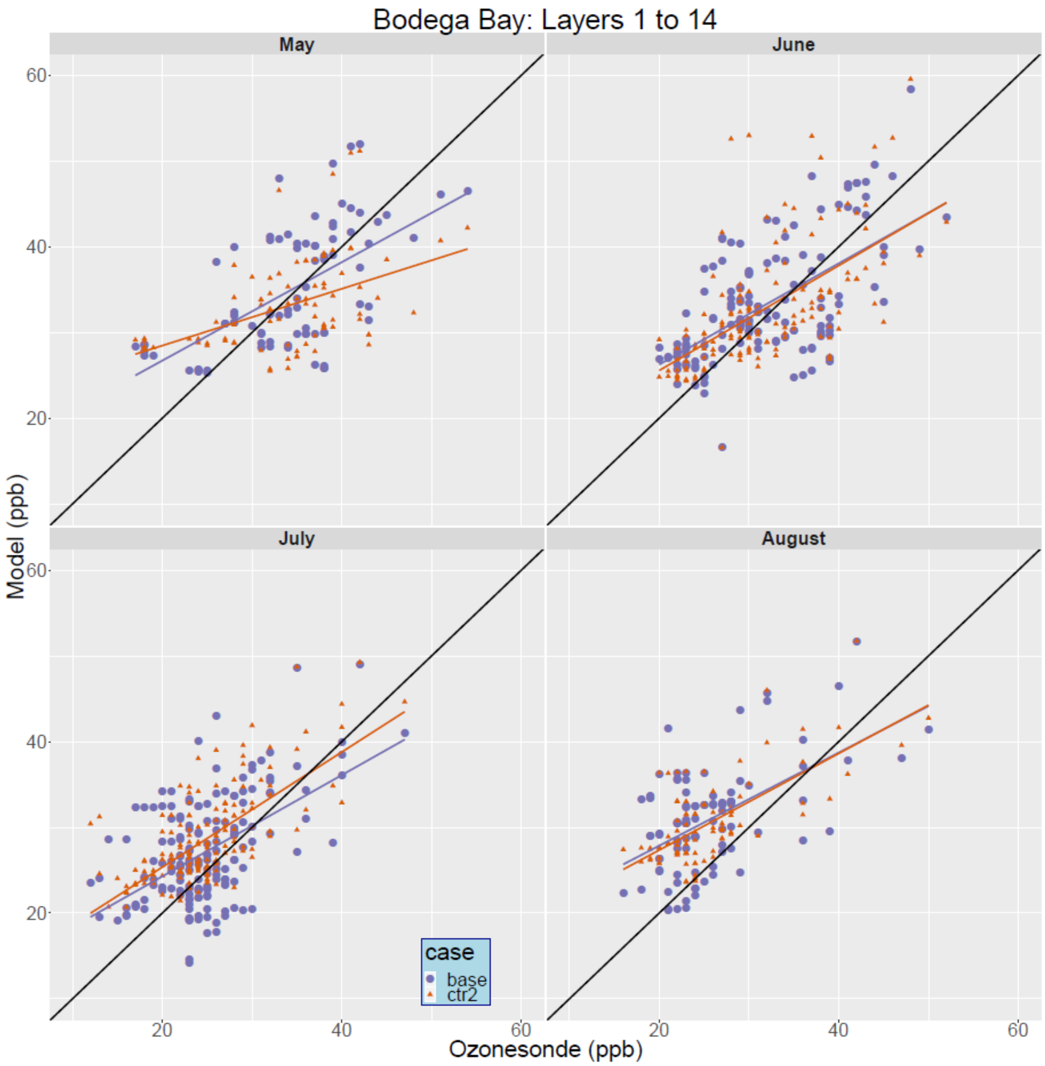

Figure 27. Scatter plots of CMAQ simulated ozone (unadjusted BC as blue circles, alternative adjusted BC as red triangles) versus ozonesonde measurements at Bodega Bay by month and collectively over CMAQ layers 1-14 (0-600 m). Linear regression lines are shown for both sets of CMAQ data; the 1:1 line is shown in black.

Table 7. Linear regression statistics by month from Figure 27.

Month	Case	Slope	Intercept	R^2
May	Unadjusted	0.574	15.2	0.37
	Adjusted	0.332	21.8	0.20
June	Unadjusted	0.590	14.4	0.36
	Adjusted	0.612	13.3	0.37
July	Unadjusted	0.591	12.4	0.27
	Adjusted	0.672	11.9	0.48
August	Unadjusted	0.543	16.9	0.30
	Adjusted	0.564	16.0	0.47

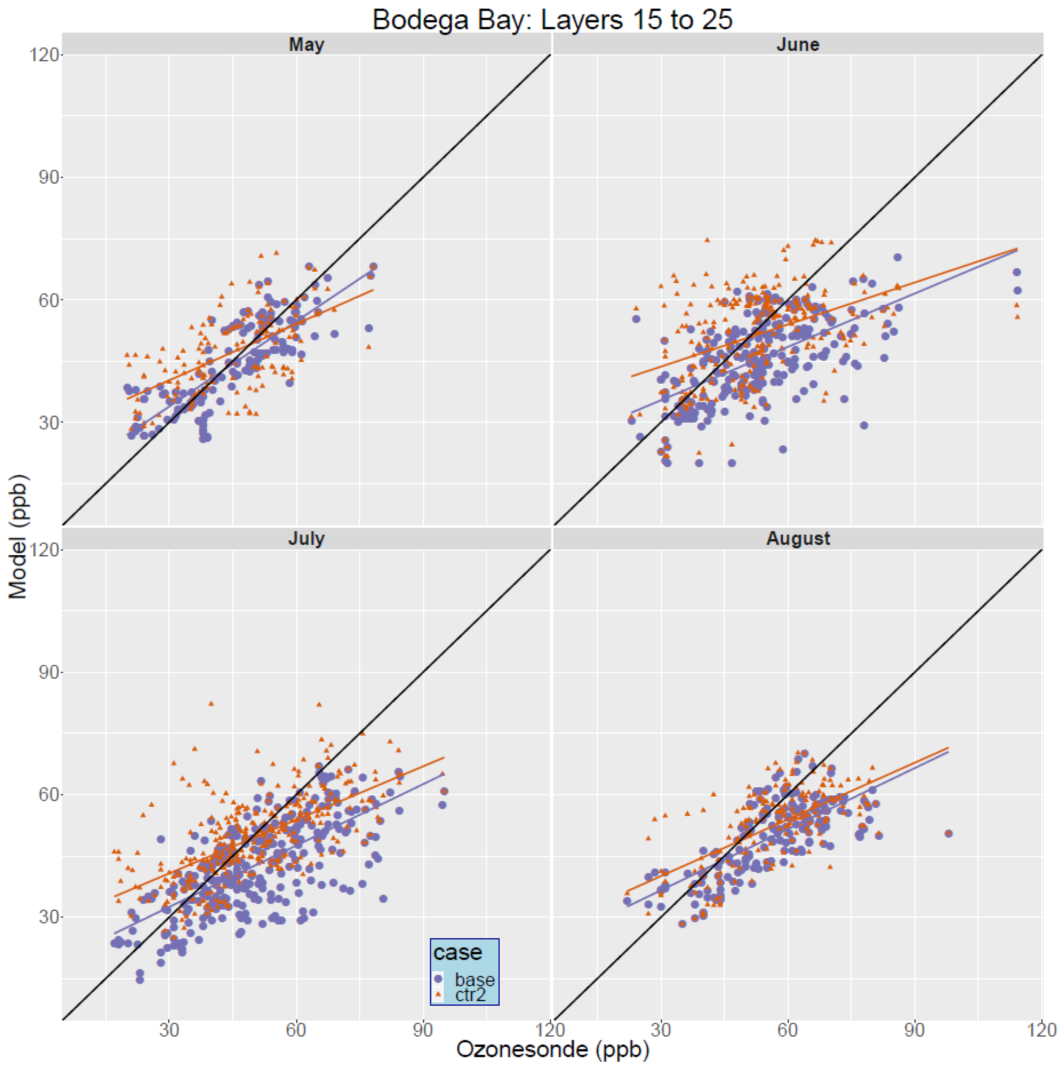

Figure 28. Scatter plots of CMAQ simulated ozone (unadjusted BC as blue circles, alternative adjusted BC as red triangles) versus ozonesonde measurements at Bodega Bay by month and collectively over CMAQ layers 15-25 (600-5000 m). Linear regression lines are shown for both sets of CMAQ data; the 1:1 line is shown in black.

Table 8. Linear regression statistics by month from Figure 28.

Month	Case	Slope	Intercept	R^2
May	Unadjusted	0.695	13.0	0.66
	Adjusted	0.571	26.4	0.36
June	Unadjusted	0.436	22.3	0.36
	Adjusted	0.370	33.3	0.20
July	Unadjusted	0.501	17.4	0.47
	Adjusted	0.422	27.6	0.40
August	Unadjusted	0.499	21.6	0.50
	Adjusted	0.474	26.1	0.39

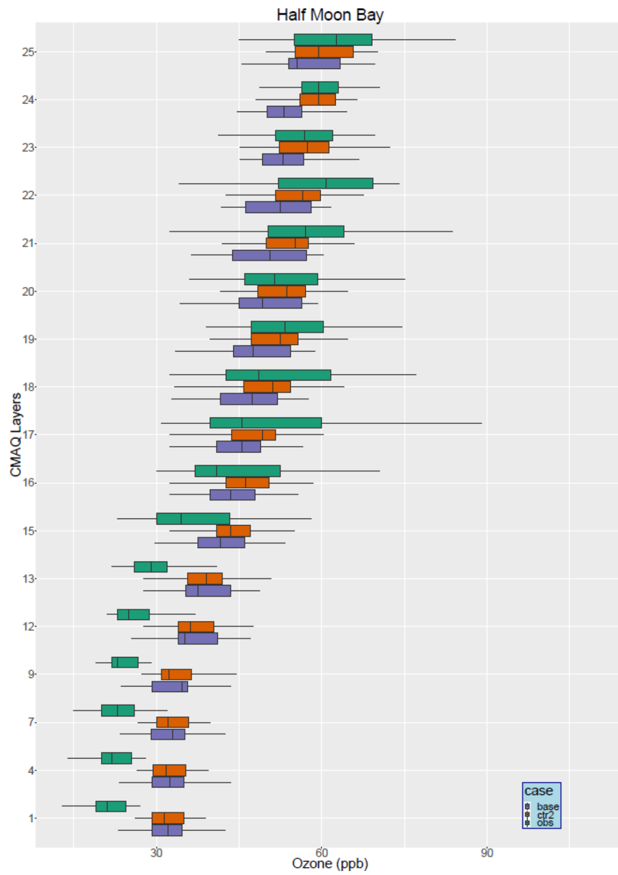

Figure 29. Comparison of July-August ozone profile distributions at Half Moon Bay: observations (green), CMAQ with unadjusted BCs (blue) and CMAQ with alternative adjusted BCs (orange). Boxes represent inter-quartile ranges, vertical lines represent medians, and whiskers represent ±1.5 times the inter-quartile range. Extreme outliers are not plotted.

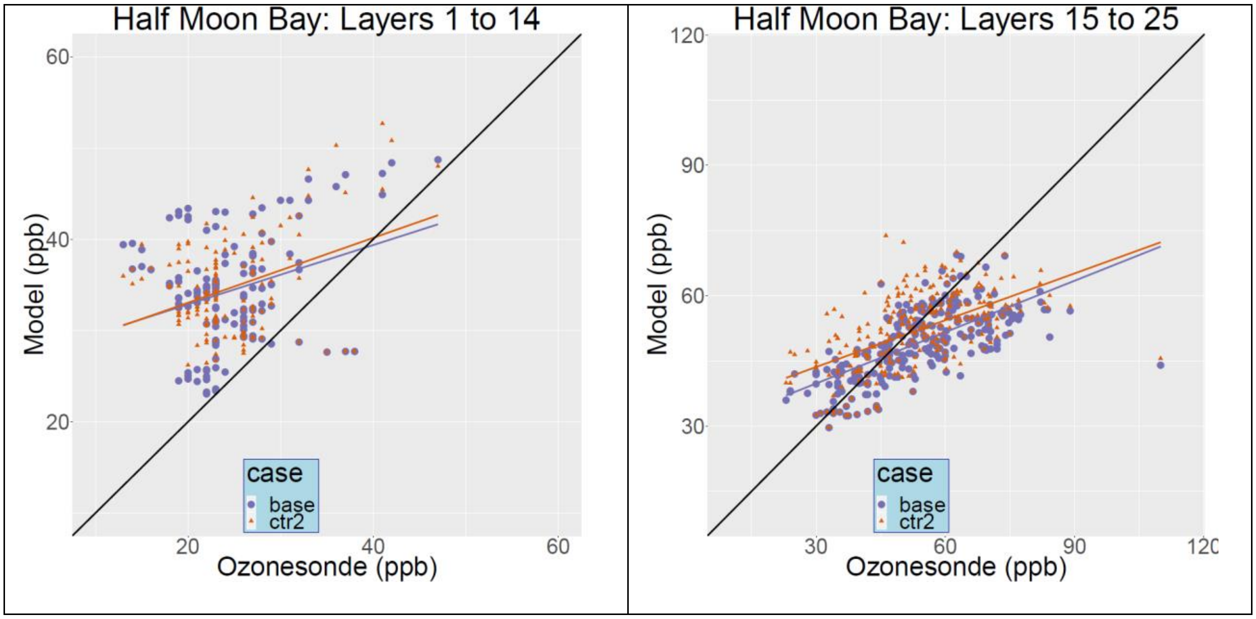

Figure 30. Scatter plots of CMAQ simulated ozone (unadjusted BC as blue circles, alternative adjusted BC as red triangles) versus ozonesonde measurements at Half Moon Bay collectively over CMAQ layers 1-14 (0-600 m, left) and 15-25 (600-5000 m, right). Linear regression lines are shown for both sets of CMAQ data; the 1:1 line is shown in black.

Table 9. Linear regression statistics by month from Figure 30.

Layers 1 to 14

Month	Case	Slope	Intercept	R^2
Jul-Aug	Unadjusted	0.325	26.3	0.09
	Adjusted	0.352	25.9	0.14

Layers 15 to 25

Month	Case	Slope	Intercept	R^2
Jul-Aug	Unadjusted	0.394	27.9	0.44
	Adjusted	0.381	32.8	0.31

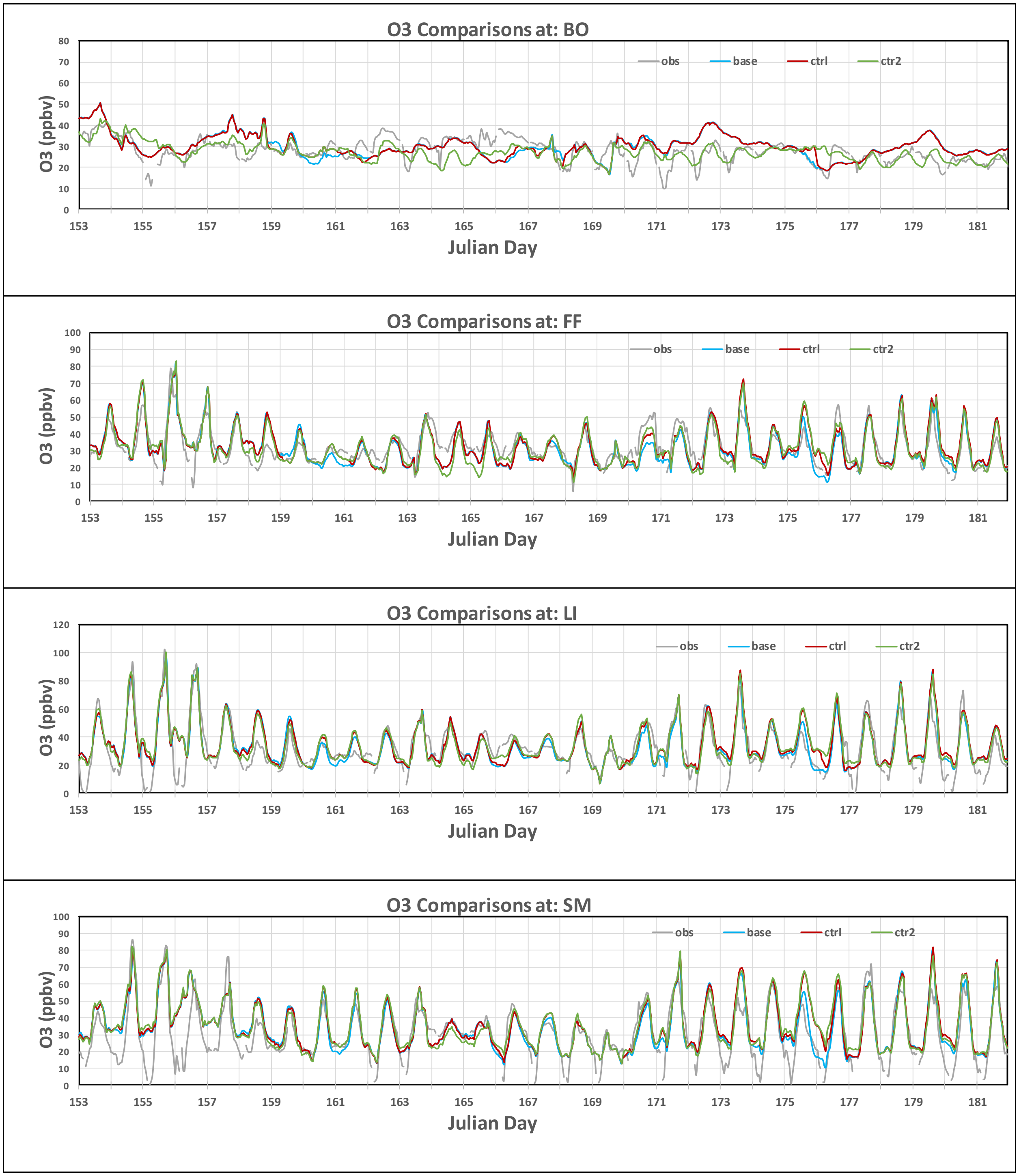

Figure 31. Time series of 1-hour ozone over June 2016 at four Bay Area sites: Bodega Bay (BO, top), Fairfield (FF, second from top), Livermore (LI, third from top), and San Martin (SM, bottom). Observations are in grey, CMAQ simulation with unadjusted ozone BCs is in blue, CMAQ simulation with original adjusted ozone BCs is in red, and CMAQ simulation with alternative adjusted ozone BCs is in green.

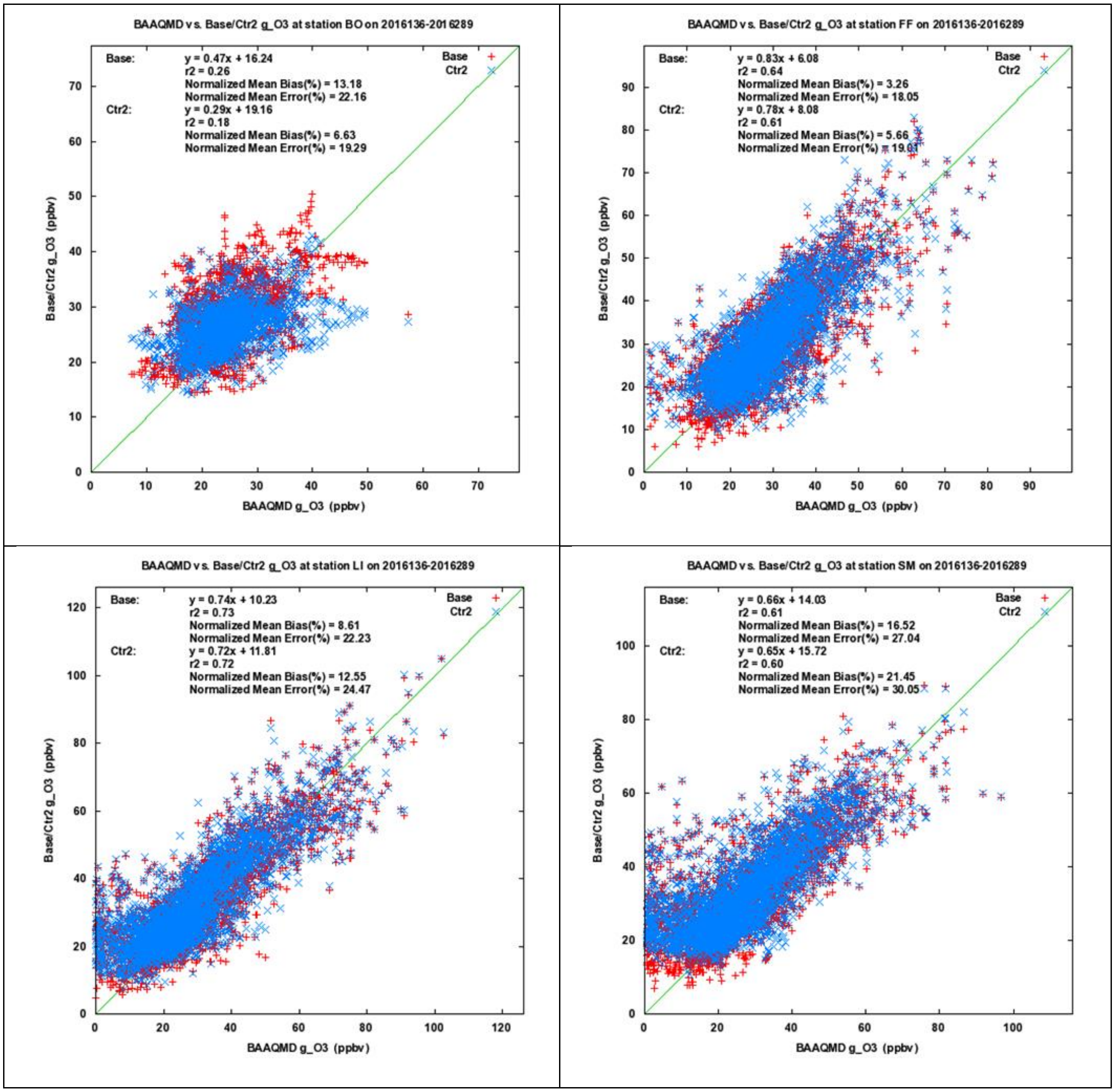

Figure 32. Scatter plots of 1-hour ozone over May-October 2016 at four Bay Area sites: Bodega Bay (BO, top left), Fairfield (FF, top right), Livermore (LI, bottom left), and San Martin (SM, bottom right). CMAQ simulation with unadjusted ozone BCs is in red, and CMAQ simulation with alternative adjusted ozone BCs is in blue. Statistics are calculated for all 1-hour observation-prediction pairings with no concentration cutoff (no floor).

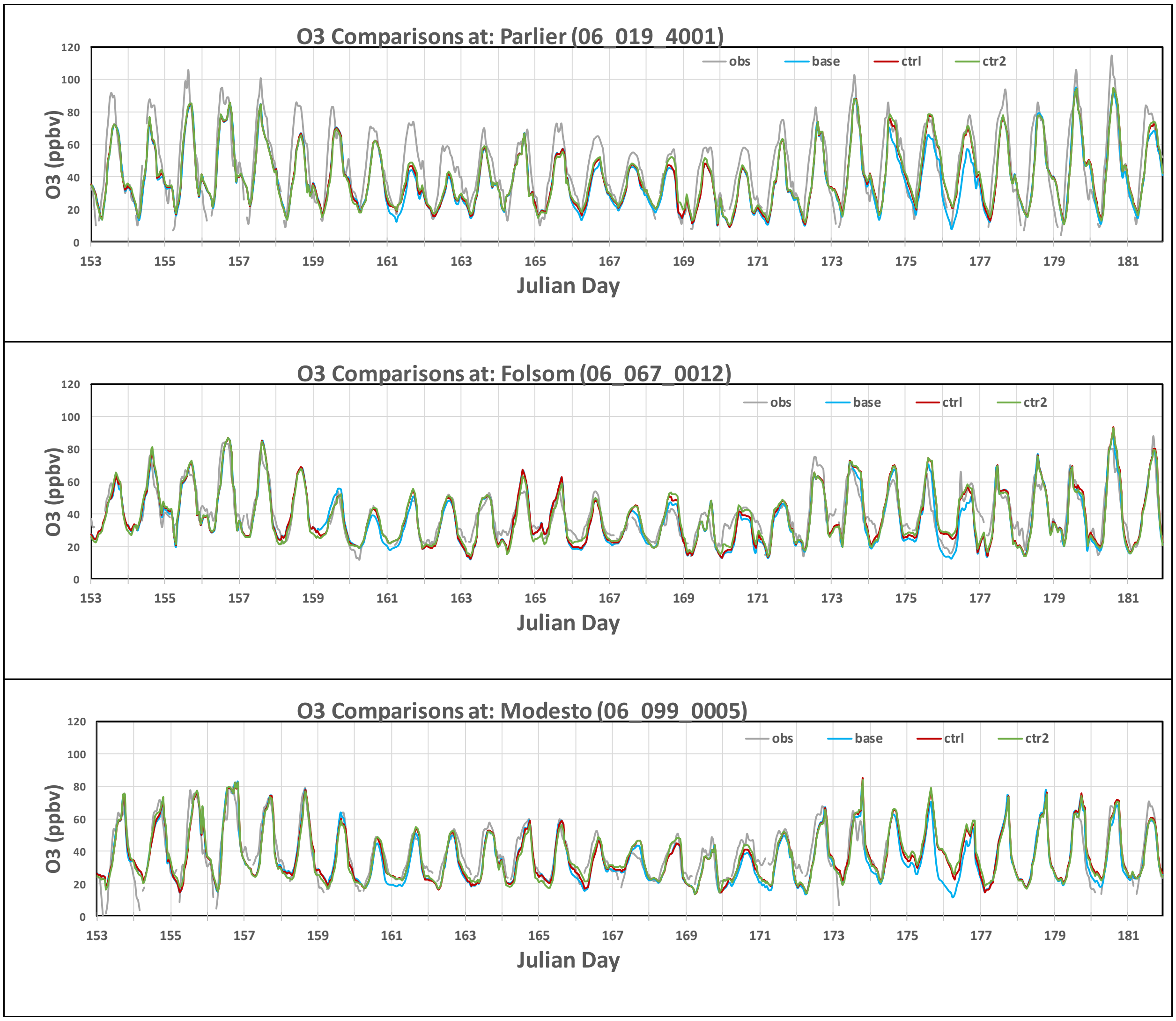

Figure 33. Time series of 1-hour ozone over June 2016 at three Central Valley sites: Parlier (top), Folsom (middle), and Modesto (bottom). Observations are in grey, CMAQ simulation with unadjusted ozone BCs is in blue, CMAQ simulation with original adjusted ozone BCs is in red, and CMAQ simulation with alternative adjusted ozone BCs is in green.

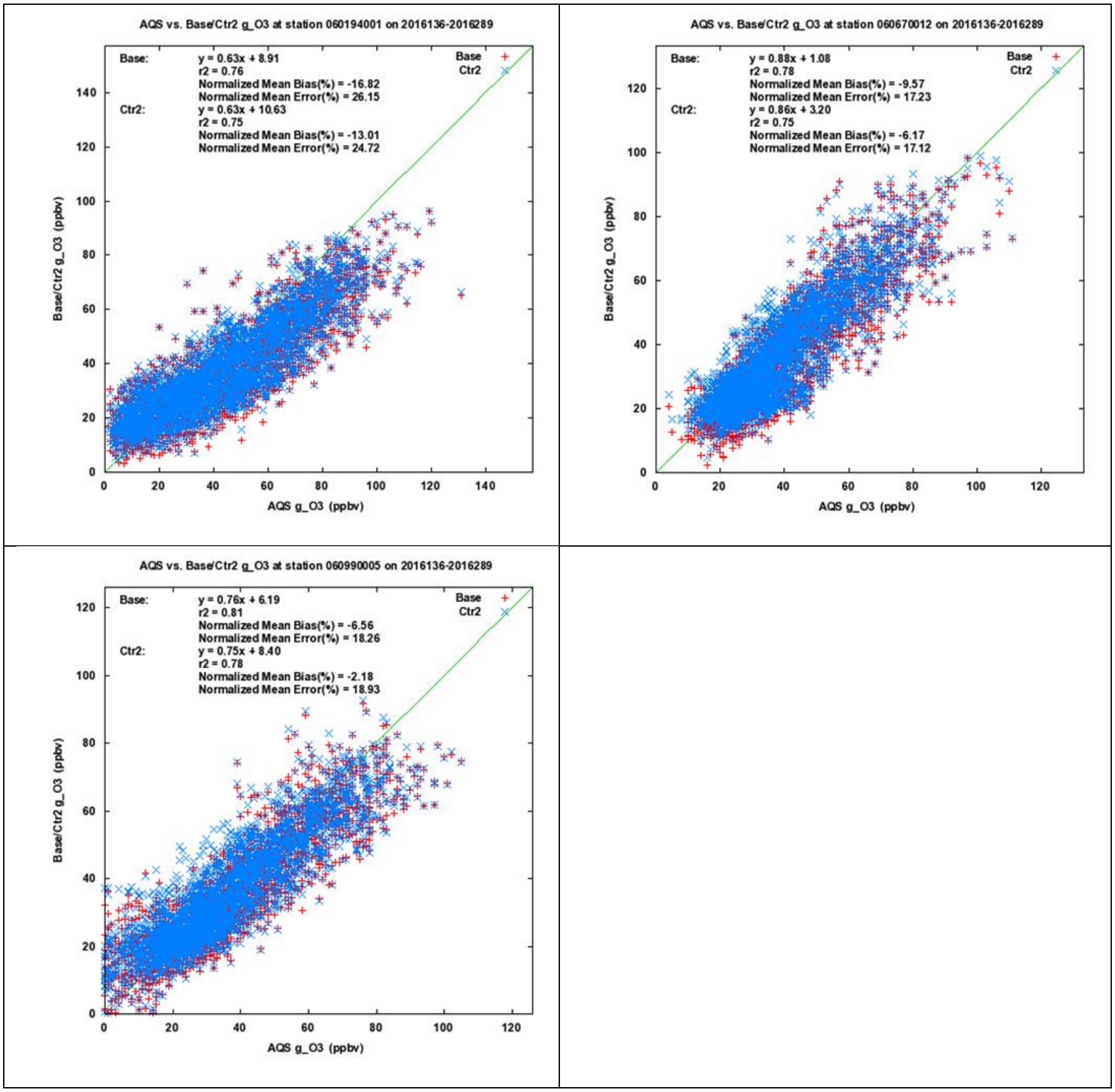

Figure 34. Scatter plots of 1-hour ozone over May-October 2016 at three Central Valley sites: Parlier (top left), Folsom (top right), and Modesto (bottom left). CMAQ simulation with unadjusted ozone BCs is in red, and CMAQ simulation with alternative adjusted ozone BCs is in blue. Statistics are calculated for all 1-hour observation-prediction pairings with no concentration cutoff (no floor).

3.6 Statistical Summary at Surface Monitoring Sites

Tables 10 through 15 list ozone statistical performance metrics (normalized bias, normalized gross error and R^2) at each of 6 surface monitoring sites analyzed in this study, for the unadjusted BC case, the initial BC adjusted case, and the alternative BC adjusted case. Three groups of statistics are shown: metrics based on all ozone observation-simulation pairs (no "cutoff", as described above), and metrics based on applying observed ozone "cutoffs" at 60 and 65 ppb to isolate model performance impacts during high ozone. Note that Bodega Bay recorded no ozone above 60 ppb throughout the period of May-October, so no statistics based on cutoffs are available for that site (see Figures 23 and 32).

When addressing only periods of high observed ozone, model gross error is slightly better at all sites compared to error over all hours (no cutoffs). This means that CMAQ performs somewhat better at simulating the higher ozone at these sites. On the other hand, model correlations (R^2) degrade substantially when cutoffs are applied because the number of observation-prediction pairings are much smaller and the scatter among those pairings increases. This is a common characteristic of these types of analyses.

Again, adjusting boundary conditions leads to only marginal statistical impacts with and without cutoffs. In fact, statistical differences between base and adjusted cases tend to be smaller with cutoffs than without. Therefore, the boundary ozone adjustments have less impact on high ozone days and more impact on low ozone days and hours of minimum ozone.

Table 10. Hourly ozone statistical performance metrics at Fairfield (northeast Bay Area) for the unadjusted BC case, the initial BC adjusted case, and the alternative BC adjusted case. Statistics are based on all ozone observation-simulation pairs (no "cutoff"), and for observed ozone "cutoffs" at 60 and 65 ppb.

		Base	Initial BC Adjustment	Alternative BC Adjustment
No Cutoff	NMB (%)	3.3	5.7	6.7
	NME (%)	18.1	18.4	19.0
	R^2	0.64	0.64	0.61
60 ppb Cutoff	NMB (%)	-10.5	-10.2	-10.1
	NME (%)	18.8	18.5	18.8
	R^2	0.01	0.01	0.02
65 ppb Cutoff	NMB (%)	-16.3	-15.8	-15.4
	NME (%)	17.2	16.7	16.3
	R^2	0.07	0.07	0.07

Table 11. Hourly ozone statistical performance metrics at Livermore (east Bay Area) for the unadjusted BC case, the initial BC adjusted case, and the alternative BC adjusted case. Statistics are based on all ozone observation-simulation pairs (no “cutoff”), and for observed ozone “cutoffs” at 60 and 65 ppb.

		Base	Initial BC Adjustment	Alternative BC Adjustment
No Cutoff	NMB (%)	8.6	11.6	12.6
	NME (%)	22.2	23.2	24.5
	R^2	0.73	0.73	0.72
60 ppb Cutoff	NMB (%)	-9.6	-8.9	-9.6
	NME (%)	13.5	13.2	13.8
	R^2	0.26	0.27	0.29
65 ppb Cutoff	NMB (%)	-11.6	-10.8	-11.0
	NME (%)	15.0	14.6	15.0
	R^2	0.25	0.25	0.25

Table 12. Hourly ozone statistical performance metrics at San Martin (south Bay Area) for the unadjusted BC case, the initial BC adjusted case, and the alternative BC adjusted case. Statistics are based on all ozone observation-simulation pairs (no “cutoff”), and for observed ozone “cutoffs” at 60 and 65 ppb.

		Base	Initial BC Adjustment	Alternative BC Adjustment
No Cutoff	NMB (%)	16.5	20.2	21.5
	NME (%)	27.0	28.7	30.1
	R^2	0.61	0.61	0.60
60 ppb Cutoff	NMB (%)	-11.3	-10.7	-10.7
	NME (%)	14.5	14.1	14.2
	R^2	0.16	0.16	0.16
65 ppb Cutoff	NMB (%)	-13.2	-12.6	-12.5
	NME (%)	15.6	15.2	15.1
	R^2	0.07	0.07	0.09

Table 13. Hourly ozone statistical performance metrics at Parlier (San Joaquin Valley) for the unadjusted BC case, the initial BC adjusted case, and the alternative BC adjusted case. Statistics are based on all ozone observation-simulation pairs (no “cutoff”), and for observed ozone “cutoffs” at 60 and 65 ppb.

		Base	Initial BC Adjustment	Alternative BC Adjustment
No Cutoff	NMB (%)	-16.8	-14.1	-13.0
	NME (%)	26.2	25.0	24.7
	R^2	0.76	0.76	0.75
60 ppb Cutoff	NMB (%)	-23.1	-21.8	-21.4
	NME (%)	23.6	22.4	22.0
	R^2	0.41	0.40	0.39
65 ppb Cutoff	NMB (%)	-23.1	-21.9	-21.5
	NME (%)	23.5	22.3	22.0
	R^2	0.34	0.33	0.33

Table 14. Hourly ozone statistical performance metrics at Folsom (Sacramento Valley) for the unadjusted BC case, the initial BC adjusted case, and the alternative BC adjusted case. Statistics are based on all ozone observation-simulation pairs (no "cutoff"), and for observed ozone "cutoffs" at 60 and 65 ppb.

		Base	Initial BC Adjustment	Alternative BC Adjustment
No Cutoff	NMB (%)	-9.6	-7.0	-6.2
	NME (%)	17.2	17.2	17.1
	R^2	0.78	0.76	0.75
60 ppb Cutoff	NMB (%)	-11.6	-10.3	-9.9
	NME (%)	14.7	13.9	13.8
	R^2	0.33	0.32	0.32
65 ppb Cutoff	NMB (%)	-12.3	-11.1	-10.9
	NME (%)	15.0	14.3	13.2
	R^2	0.29	0.28	0.28

Table 15. Hourly ozone statistical performance metrics at Modesto (San Joaquin Valley) for the unadjusted BC case, the initial BC adjusted case, and the alternative BC adjusted case. Statistics are based on all ozone observation-simulation pairs (no "cutoff"), and for observed ozone "cutoffs" at 60 and 65 ppb.

		Base	Initial BC Adjustment	Alternative BC Adjustment
No Cutoff	NMB (%)	-6.6	-3.3	-2.2
	NME (%)	18.3	18.4	18.9
	R^2	0.81	0.79	0.78
60 ppb Cutoff	NMB (%)	-13.5	-12.5	-12.4
	NME (%)	15.3	14.6	14.5
	R^2	0.20	0.20	0.20
65 ppb Cutoff	NMB (%)	-15.4	-14.4	-14.2
	NME (%)	16.7	15.9	15.8
	R^2	0.14	0.14	0.13

4.0 CONCLUSION

With rising contributions from international transport, regional and continental modeling boundary conditions take on increasing importance in characterizing non-US contributions and influences, particularly in the western US. Ramboll and the BAAQMD developed and applied a method to reduce regional biases in global model-derived ozone fields over the northeastern Pacific Ocean using routine ozonesonde measurements. The method was codified into a distributable software tool that can be used to adjust regional ozone boundary conditions derived from the MOZART global model over the period 2012-2016 for modeling domains extending beyond the US west coast.

Based on a 5-year compilation of daily MOZART output and ozonesonde data from Trinidad Head, the BAAQMD conducted a statistical classification analysis from which to derive a regression-based parameterized model that reduces MOZART-measurement biases on a daily basis. Ramboll then developed a file of adjusted ozone concentration profiles for each day of the 2012-2016 period for use in a Python-based tool that replaces ozone values in CMAQ boundary condition files within user-defined portions of the model domain. Ramboll developed the adjustment program to be flexible so that adjustments from regression models developed for other years can be readily incorporated in the future.

The BAAQMD applied the adjustment tool to their 2016 daily CMAQ ozone boundary condition input files. In an initial test, the BC adjustment tool was applied to the northern half of the western boundary over layers 1-25 (surface to ~5000 m); no other boundaries or layers were modified. In an alternative test, the BC adjustment was applied to the northern two-thirds of the western boundary and to the western one-third of the northern boundary (same vertical adjustment). Results from the unadjusted and both adjusted BC runs were graphically and statistically compared to 2016 CABOTS ozonesonde data and to routine surface monitoring data over the ozone season (May-October). Two basic paradigms were identified: (1) Increased BCs aloft mix down during the day over high-elevation topography, then disperse at the surface to other area of the domain; (2) reduced BCs in the marine boundary layer are transported along the coastline in the consistent northwesterly flow and occasionally drawn through coastal topographic gaps such as the Bay Area.

With respect to ozonesonde comparisons, BC adjustments had little impact on CMAQ ozone overpredictions in the marine boundary layer, which may be related to insufficient ozone destruction from oceanic halogens. However, BC adjustments did reduce ozone underpredictions aloft by better aligning modeled and observed monthly-medians, although the simulated ozone range was much smaller than observed, as would be expected with the regression model’s attempt to adjust BC ozone toward seasonal means. Overall, impacts to statistical performance throughout the ozonesonde column were minor. The Half Moon Bay ozonesonde tended to be less influenced by the choice of ozone BCs than the more northern Bodega Bay site, which may be caused by a somewhat stronger local influence from the Bay Area and/or more influence from unadjusted portions of the western boundary.

With respect to surface monitor comparisons in the Bay Area, the effects of the ozone BC adjustment were rather small and difficult to differentiate except for a few scattered days, with a tendency for more evident impacts at the inland and southern Bay Area sites. The adjusted ozone BC simulation slightly raised ozone, thereby raising the overprediction bias and gross error by a few percentage points. Similarly small impacts were evident at the Central valley sites: the adjusted ozone BC simulation slightly raised ozone, thereby improving the underprediction bias by a few percentage points. Overall, however, we found no significant change in model performance statistics or CMAQ's characterization of hourly ozone with the ozone BC adjustment. Results suggest that areas in elevated terrain along the western US coast may be more affected by boundary condition adjustments than low-level sites. Ozone levels in 2016 were relatively low compared to other years, and BC adjustments may have larger or smaller impacts in other years.

Prior to this project, the BAAQMD ran a CMAQ test wherein MOZART-based ozone boundary conditions were replaced with daily ozonesonde data from the CABOTS HMB site over July 15 – August 17, 2016. Averaged over Bay Area monitoring sites, the HMB-based boundary conditions resulted in 2-5 ppb higher ozone at all hours of the month-long simulation, which are markedly higher than we see in our results. This raises the following question: is the Trinidad Head site too far north of the Bay Area to adequately represent western boundary conditions from the eastern Pacific Ocean, and/or is the once-per-week launch schedule too infrequent to adequately adjust MOZART-derived boundary conditions?

The tool developed in this project is now available to further investigate and test additional boundary condition modifications and adjustments. The use of global models such as MOZART to derive regional BCs is much more effective and promising than previous approaches based entirely on simplistic assumptions or limited observational data. However, global models introduce their own biases and errors when their results are down-scaled for regional modeling applications. Our approach to remove these biases using a mix of model and observational data, while effective to first order, also reduces concentration variability at all altitudes (i.e., higher-order structures). Furthermore, regional model performance may be more affected by the proximity of boundary conditions to the western shoreline. We recommend future work that locates grid boundaries farther away from the coastline to minimize BC impacts. The tool developed in this project can help determine regional model sensitivity to boundary placement.

5.0 REFERENCES

Emery, C. Z. Liu, A.G. Russell, M.T. Odman, G. Yarwood, N. Kumar, 2016. Recommendations on statistics and benchmarks to assess photochemical model performance, *Journal of the Air & Waste Management Association*, DOI: 10.1080/10962247.2016.1265027.

Emmons, L. K., Walters, S., Hess, P. G., Lamarque, J.-F., Pfister, G. G., Fillmore, D., Granier, C., Guenther, A., Kinnison, D., Laepple, T., Orlando, J., Tie, X., Tyndall, G., Wiedinmyer, C., Baughcum, S. L., and Kloster, S., 2010. Description and evaluation of the Model for Ozone and Related chemical Tracers, version 4 (MOZART-4), *Geosci. Model Dev.*, 3, 43-67, https://doi.org/10.5194/gmd-3-43-2010.

Marsh, D.R., M.J. Mills, D.E. Kinnison, J.-F. Lamarque, N. Calvo, L.M. Polvani, 2013. Climate Change from 1850 to 2005 Simulated in CESM1(WACCM), J. Climate, 26, 7372-7391, DOI: 10.1175/JCLI-D-12-00558.1.

NOAA, 2019. https://www.esrl.noaa.gov/gmd/ozwv/ozsondes/.

UC Davis, 2018. CABOTS UCD Aircraft Analysis. Presented at the California Baseline Ozone Transport Study (CABOTS) Science Meeting, 27 February 2018.